

## Articles

## Synthesis and Characterization of Titanium Complexes Bearing Two $\beta$ -Enaminoketonato Ligands with Electron-Withdrawing Groups and Their Behavior in Ethylene Polymerization

Wei-Ping Ye,<sup>†,‡</sup> Jie Zhan,<sup>†,‡</sup> Li Pan,<sup>†</sup> Ning-Hai Hu, and Yue-Sheng Li<sup>\*,†</sup>

State Key Laboratory of Polymer Physics and Chemistry, Changchun Institute of Applied Chemistry, Chinese Academy of Sciences, Changchun 130022, People's Republic of China, and Graduate School of the Chinese Academy of Sciences, Changchun Branch, People's Republic of China

Received August 6, 2007

A series of new titanium complexes with two asymmetric bidentate  $\beta$ -enaminoketonato (N,O) ligands (**4b–t**),  $[\text{RN}=\text{C}(\text{CF}_3)\text{CHC}(t\text{-Bu})\text{O}]_2\text{TiCl}_2$  (**4b**, R =  $-\text{C}_6\text{H}_4\text{F}(o)$ ; **4c**, R =  $-\text{C}_6\text{H}_4\text{F}(m)$ ; **4d**, R =  $-\text{C}_6\text{H}_4\text{F}(p)$ ; **4e**, R =  $-\text{C}_6\text{H}_3\text{F}_2(2,3)$ ; **4f**, R =  $-\text{C}_6\text{H}_3\text{F}_2(2,4)$ ; **4g**, R =  $-\text{C}_6\text{H}_3\text{F}_2(2,5)$ ; **4h**, R =  $-\text{C}_6\text{H}_3\text{F}_2(2,6)$ ; **4i**, R =  $-\text{C}_6\text{H}_3\text{F}_2(3,4)$ ; **4j**, R =  $-\text{C}_6\text{H}_3\text{F}_2(3,5)$ ; **4k**, R =  $-\text{C}_6\text{H}_2\text{F}_3(2,3,4)$ ; **4l**, R =  $-\text{C}_6\text{H}_2\text{F}_3(3,4,5)$ ; **4m**, R =  $-\text{C}_6\text{H}_4\text{CF}_3(o)$ ; **4n**, R =  $-\text{C}_6\text{H}_4\text{CF}_3(m)$ ; **4o**, R =  $-\text{C}_6\text{H}_4\text{CF}_3(p)$ ; **4p**, R =  $-\text{C}_6\text{H}_4\text{Cl}(p)$ ; **4q**, R =  $-\text{C}_6\text{H}_4\text{I}(p)$ ; **4r**, R =  $-\text{C}_6\text{H}_4\text{NO}_2(p)$ ; **4s**, R =  $-\text{CH}_2\text{C}_6\text{H}_5$ ; **4t**, R =  $-\text{C}_6\text{H}_{11}$ ), have been synthesized and characterized. X-ray crystal structures suggest that complexes **4a–d**, **4j**, and **4m** all adopt a distorted octahedral geometry around the titanium centers. Two chlorine atoms in complexes **4a–d** and **4j** are in *cis*-configuration, while those of complex **4m** are *trans*. NMR spectra and X-ray structure analyses reveal that the conformational isomers of some complexes, such as **4b**, in which the two  $\beta$ -enaminoketonato ligands bear asymmetrical N-phenyl rings, exist both in solution and in solid state. With modified methylaluminoxane (MMAO) as a cocatalyst, complexes **4b–l** and **4n–q** are highly active toward ethylene polymerization and produce high molecular weight polyethylenes. The catalytic activities are significantly enhanced by introducing electron-withdrawing groups (EWG), such as fluorine and chlorine atom(s) or the trifluoromethyl group, into suitable positions on the N-aryl rings. The titanium complex **4m** is inactive toward ethylene polymerization due to the *trans*-configuration of the two chlorine atoms. In addition, the titanium complexes display low catalytic activity for ethylene polymerization only if the N-substituents are not aromatic.

### Introduction

In recent years, significant attention has focused on the design and synthesis of highly active, well-defined or single-site transition metal catalysts for olefin polymerization.<sup>1</sup> After the extensive investigation of the transition metal complexes with cyclopentadienyl (Cp) or derivate ligands, the new non-Cp ligand environment has currently attracted more and more interest,<sup>2–9</sup> which brought about the discovery of a variety of non-metallocene catalysts. For example, Brookhart and co-

workers developed nickel and palladium catalysts based on chelating diimine ligands,<sup>10</sup> Grubbs and his colleagues reported neutral nickel catalysts based on chelating phenoxyimine ligands,<sup>11</sup> Brookhart and Gibson reported independently iron and cobalt catalysts based on chelating diimine-pyridine ligands,<sup>12,13</sup> and Fujita and Coates discovered titanium and zirconium catalysts based on chelating phenoxyimine ligands.<sup>14,15</sup> This research promoted the development of a non-metallocene catalyst for olefin polymerization. Subsequent research demonstrated that subtle variation of the ligands, including steric

\* To whom correspondence should be addressed. Fax: +86-431-5262124. E-mail: ysl@ciac.jl.cn.

<sup>†</sup> State Key Laboratory of Polymer Physics and Chemistry.

<sup>‡</sup> Graduate School of the Chinese Academy of Sciences.

(1) (a) Britovsek, G. J. P.; Gibson, V. C.; Wass, D. F. *Angew. Chem., Int. Ed.* **1999**, *38*, 428. (b) Ittel, S. D.; Johnson, L. K.; Brookhart, M. *Chem. Rev.* **2000**, *100*, 1169. (c) Gibson, V. C.; Stefan, S. K. *Chem. Rev.* **2003**, *103*, 283.

(2) Domsikia, G. J.; Rose, J. M.; Coates, G. W.; Bolig, A. D.; Brookhart, M. *Prog. Polym. Sci.* **2007**, *32*, 30.

(3) Ferreira, M. J.; Martins, A. M. *Coord. Chem. Rev.* **2006**, *250*, 118.

(4) Nomura, K.; Liu, J. Y.; Padmanabhan, S.; Kitiyanan, B. *J. Mol. Catal. A: Chem.* **2007**, *267*, 1.

(5) Mitani, M.; Nakano, T.; Fujita, T. *Chem.–Eur. J.* **2003**, *9*, 2397.

(6) (a) Wang, C.; Ma, Z.; Sun, X. L.; Gao, Y.; Guo, Y. H.; Tang, Y.; Shi, L. P. *Organometallics* **2006**, *25*, 3259. (b) Li, W.; Sun, H.; Chen, M.; Wang, Z.; Hu, D.; Shen, Q.; Zhang, Y. *Organometallics* **2005**, *24*, 5925. (c) Wang, C.; Sun, X. L.; Guo, Y. H.; Gao, Y.; Liu, B.; Ma, Z.; Xia, W.; Shi, L. P.; Tang, Y. *Macromol. Rapid Commun.* **2005**, *26*, 1609.

(7) Xu, T.; Mu, Y.; Gao, W.; Ni, J.; Ye, L.; Tao, Y. *J. Am. Chem. Soc.* **2007**, *129*, 2236.

(8) Long, R. J.; Gibson, V. C.; White, A. J. P.; Williams, D. J. *Inorg. Chem.* **2006**, *45*, 511–513.

(9) Beckerle, K.; Manivannan, R.; Spaniol, T. P.; Okuda, J. *Organometallics* **2006**, *25*, 3019.

(10) (a) Johnson, L. K.; Killian, C. M.; Brookhart, M. *J. Am. Chem. Soc.* **1995**, *117*, 6414. (b) Johnson, L. K.; Mecking, S.; Brookhart, M. *J. Am. Chem. Soc.* **1996**, *118*, 267. (c) Killian, C. M.; Tempel, D. J.; Johnson, L. K.; Brookhart, M. *J. Am. Chem. Soc.* **1996**, *118*, 11664. (d) Gates, D. P.; Svejda, S. A.; Onate, E.; Killian, C. M.; Johnson, L. K.; White, P. S.; Brookhart, M. *Macromolecules* **2000**, *33*, 2320.

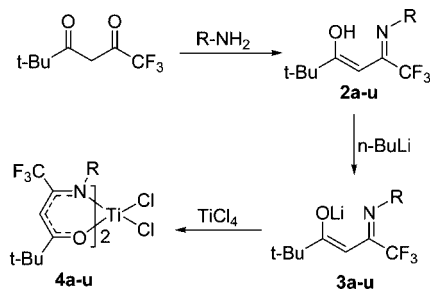
(11) (a) Wang, C.; Friedrich, A.; Younkin, T. R.; Li, R. T.; Grubbs, R. H.; Bansleben, A.; Day, M. W. *Organometallics* **1998**, *17*, 3149. (b) Younkin, T. R.; Connor, E. F.; Henderson, J. I.; Friedrich, S. K.; Grubbs, R. H.; Bansleben, A. *Science* **2000**, *287*, 460.

(12) Small, B. L.; Brookhart, M.; Bennett, A. A. *J. Am. Chem. Soc.* **1998**, *120*, 4049.

and electronic effects, can greatly influence the performance of catalysts in olefin polymerization. For example, Mazzeo and co-workers found that the isotacticities of the polypropenes obtained by a series of titanium catalysts bearing phenoxyimine ligands were considerably influenced by the *o*-phenoxy halide substituents.<sup>16</sup> Tang and his colleagues reported a series of titanium complexes bearing monoanionic tridentate ligands and found their polymerization behavior for olefins was also greatly influenced by the ligand structure.<sup>6a</sup> Especially, Fujita and Coates found that the polymerization behavior of the titanium catalysts bearing phenoxyimine ligands were obviously influenced by introducing fluorine atom(s) to the ligands: catalytic activity increased with increasing number of fluorine atoms, and only the titanium complexes with fluorine atom(s) adjacent to the imine nitrogen promoted living ethylene polymerization under similar conditions.<sup>14c,15c</sup>

Recently we reported a type of titanium catalyst with chelating asymmetrical bidentate  $\beta$ -enaminoketonato ligands, [PhNC(R<sub>2</sub>)C(H)C(R<sub>1</sub>)O]<sub>2</sub>TiCl<sub>2</sub>, for olefin polymerization.<sup>17</sup> As the  $\beta$ -enaminoketonato ligand has multiple sites for introducing or changing the substituents, the steric and electronic requirements of the metal center can be modulated easily by varying the ligand structure. By variation of the substituents (R<sub>1</sub> and R<sub>2</sub>), we obtained a series of highly efficient catalysts toward ethylene polymerization and ethylene/ $\alpha$ -olefin or cycloolefin copolymerizations.<sup>18</sup> Among all the catalysts studied, catalyst **4a** (R<sub>1</sub> = *t*-Bu, R<sub>2</sub> = CF<sub>3</sub>) showed the highest activity under the same conditions. The fact that the variation of the ligand structure may lead to profound changes in the performance of the catalyst and the properties of the polymers prompts us to synthesize new titanium complexes [(EWG)ArN=C(CF<sub>3</sub>)CHC(*t*-Bu)O]<sub>2</sub>TiCl<sub>2</sub> by introducing the fluorine atoms or other EWG to the  $\beta$ -enaminoketonato ligands and investigate the effect of these EWGs on the polymerization behavior of olefins. Herein, we describe the synthesis, characterization, and ethylene polymerization behavior of these titanium complexes bearing aromatic-substituted  $\beta$ -enaminoketonato ligands.

### Scheme 1. General Synthetic Route of the Titanium Complexes Used in This Study



a: R = -C <sub>6</sub> H <sub>5</sub>	h: R = -C <sub>6</sub> H <sub>3</sub> F <sub>2</sub> (2,6)	o: R = -C <sub>6</sub> H <sub>4</sub> CF <sub>3</sub> ( <i>p</i> )
b: R = -C <sub>6</sub> H <sub>4</sub> F( <i>o</i> )	i: R = -C <sub>6</sub> H <sub>3</sub> F <sub>2</sub> (3,4)	p: R = -C <sub>6</sub> H <sub>4</sub> Cl( <i>p</i> )
c: R = -C <sub>6</sub> H <sub>4</sub> F( <i>m</i> )	j: R = -C <sub>6</sub> H <sub>3</sub> F <sub>2</sub> (3,5)	q: R = -C <sub>6</sub> H <sub>4</sub> ( <i>p</i> )
d: R = -C <sub>6</sub> H <sub>4</sub> F( <i>p</i> )	k: R = -C <sub>6</sub> H <sub>2</sub> F <sub>3</sub> (2,3,4)	r: R = -C <sub>6</sub> H <sub>4</sub> NO <sub>2</sub> ( <i>p</i> )
e: R = -C <sub>6</sub> H <sub>3</sub> F <sub>2</sub> (2,3)	l: R = -C <sub>6</sub> H <sub>2</sub> F <sub>3</sub> (3,4,5)	s: R = -CH <sub>2</sub> C <sub>6</sub> H <sub>5</sub>
f: R = -C <sub>6</sub> H <sub>3</sub> F <sub>2</sub> (2,4)	m: R = -C <sub>6</sub> H <sub>4</sub> CF <sub>3</sub> ( <i>o</i> )	t: R = -C <sub>6</sub> H <sub>11</sub>
g: R = -C <sub>6</sub> H <sub>3</sub> F <sub>2</sub> (2,5)	n: R = -C <sub>6</sub> H <sub>4</sub> CF <sub>3</sub> ( <i>m</i> )	u: R = -C <sub>6</sub> H <sub>4</sub> Me

## Results and Discussion

**Synthesis and Characterization of New Titanium Complexes.** New titanium complexes **4b–q** used here were synthesized according to the modified procedures reported previously as shown in Scheme 1.<sup>17</sup>  $\beta$ -Enaminoketonates **2b–s** were obtained in moderate to high yields (**2b**, 58%; **2c**, 69%; **2d**, 75%; **2e**, 71%; **2f**, 61%; **2g**, 74%; **2h**, 64%; **2i**, 72%; **2j**, 80%; **2k**, 78%; **2l**, 62%; **2m**, 67%; **2n**, 79%; **2o**, 82%; **2p**, 86%; **2q**, 59%; **2r**, 57%; **2s**, 46%) by the condensation of 1,1,1-trifluoro-5,5-dimethyl-2,4-hexanedione with the corresponding aniline derivatives in toluene containing a little *p*-toluenesulfonic acid as a catalyst.  $\beta$ -Enaminoketonate **2t** was not obtained via the same method probably due to the strong basicity of cyclohexylamine and the strong acidity of the  $\beta$ -diketonate. This compound was prepared in poor yield (35%) by the reaction of the  $\beta$ -diketonate with cyclohexylamine in toluene using TiCl<sub>4</sub> as a catalyst. The titanium complexes **4b–t** were prepared under moderate conditions in good yields (**4b**, 67%; **4c**, 78%; **4d**, 76%; **4e**, 73%; **4f**, 84%; **4g**, 65%; **4h**, 80%; **4i**, 67%; **4j**, 65%; **4k**, 67%; **4l**, 70%; **4m**, 76%; **4n**, 82%; **4o**, 86%; **4p**, 71%; **4q**, 76%; **4r**, 66%; **4s**, 73%; **4t**, 61%) by the reaction of TiCl<sub>4</sub> with 2 equiv of the lithium salts of  $\beta$ -enaminoketonato **3b–t** in dry diethyl ether. The resulting complexes were obtained as dark red crystalline solids.

The chelate complexes [O,N]<sub>2</sub>TiCl<sub>2</sub> probably exist as five configurational isomers, as shown in Scheme 2. The relative formation energies (RFE) of these isomers were calculated using density functional theory (DFT) for the representative complexes, **4a–d**, **4m**, and **4n**, and are summarized in Table 1. The data listed in Table 1 indicate that the isomer *cis-I*, of all the complexes except for **4m**, in which two oxygen atoms are *trans*, and the two nitrogen atoms and two chlorine atoms are in *cis* positions, displays the lowest RFE and is the most stable. However, for complex **4m**, isomer *trans-II*, in which two oxygen atoms, two nitrogen atoms, and two chlorine atoms are all in *trans* configuration, displays the lowest RFE and is the most stable. This result could be caused by the large volume of the *ortho*-trifluoromethyl groups on the N-aryl moieties. These calculated results are further confirmed by crystallographic analyses.

The molecular structures of complexes **4a–d**, **4j**, and **4m** were confirmed by single-crystal X-ray structure analyses.

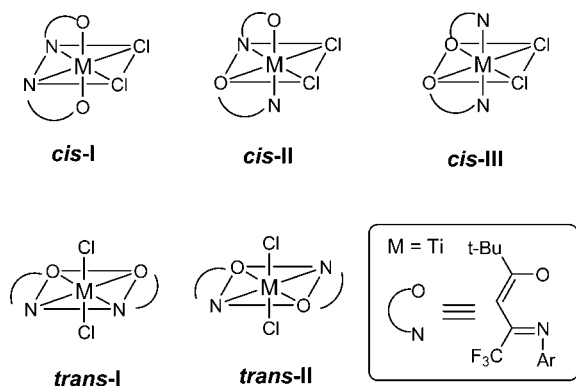
(13) (a) Britovsek, G. P. J.; Gibson, V. C.; Kimberley, B. S.; Maddox, P. J.; McTavish, S. J.; Solan, G. A.; White, A. J. P.; Williams, D. J. *Chem. Commun.* **1998**, 849. (b) Britovsek, G. J. P.; Bruce, M.; Gibson, V. C.; Kimberley, B. S.; Maddox, P. J.; Mastroianni, S. S.; McTavish, J.; Redshaw, C.; Solan, G. A.; Strömberg, S.; White, A. J. P.; Williams, D. J. *J. Am. Chem. Soc.* **1999**, *121*, 8728.

(14) (a) Saito, J.; Mitani, M.; Mohri, J.; Yoshida, Y.; Mastui, S.; Ishii, S.; Kojoh, S.; Kashiwa, N.; Fujita, T. *Angew. Chem., Int. Ed.* **2001**, *40*, 2918. (b) Matsui, S.; Mitani, M.; Saito, J.; Tohi, Y.; Makio, H.; Matsukawa, N.; Takagi, Y.; Tsuru, K.; Nitabar, M.; Nakano, T.; Tanaka, H.; Kashiwa, N.; Fujita, T. *J. Am. Chem. Soc.* **2001**, *123*, 6847. (c) Mitani, M.; Mohri, J.; Yoshida, Y.; Saito, J.; Ishii, S.; Tsuru, K.; Matsui, S.; Furuyama, R.; Nakano, T.; Tanaka, H.; Kojoh, S.-I.; Matsugi, T.; Kashiwa, N.; Fujita, T. *J. Am. Chem. Soc.* **2002**, *124*, 3327. (d) Mitani, M.; Furuyama, R.; Mohri, J.; Saito, J.; Ishii, S.; Terao, H.; Kashiwa, N.; Fujita, T. *J. Am. Chem. Soc.* **2002**, *124*, 7888. (e) Mitani, M.; Furuyama, R.; Mohri, J.; Saito, J.; Ishii, S.; Terao, H.; Nakano, T.; Tanaka, H.; Fujita, T. *J. Am. Chem. Soc.* **2003**, *125*, 4293.

(15) (a) Tian, J.; Hustad, P. D.; Coates, G. W. *J. Am. Chem. Soc.* **2001**, *123*, 5134. (b) Hustad, P. D.; Coates, G. W. *J. Am. Chem. Soc.* **2002**, *124*, 11578. (c) Mason, A. F.; Tian, J.; Hustad, P. D.; Lobkovsky, E. B.; Coates, G. W.; Israel, J. *Chem.* **2002**, *42*, 301. (d) Reinartz, S.; Mason, A. F.; Lobkovsky, E. B.; Coates, G. W. *Organometallics* **2003**, *22*, 2542. (e) Mason, A. F.; Coates, G. W. *J. Am. Chem. Soc.* **2004**, *126*, 10798. (f) Mason, A. F.; Coates, G. W. *J. Am. Chem. Soc.* **2004**, *126*, 16326.

(16) Mazzeo, M.; Strianese, M.; Lamberti, M.; Santoriello, I.; Pellicchia, C. *Macromolecules* **2006**, *39*, 7812–7820.

(17) (a) Li, X. F.; Dai, K.; Ye, W. P.; Pan, L.; Li, Y. S. *Organometallics* **2004**, *23*, 1223. (b) Tang, L. M.; Hu, T.; Bo, Y. J.; Li, Y. S.; Hu, N. H. *J. Organomet. Chem.* **2005**, *690*, 3135.

**Scheme 2. Structures of Five Configurational Isomers of the Titanium Complex**


Crystals suitable for X-ray diffraction were grown from hexane solutions at  $-20\text{ }^{\circ}\text{C}$ . The crystallographic data together with the collection and refinement parameters are summarized in Table 2. The molecular structures of **4a**, **4b**, and **4m** are shown in Figures 1–3; **4c**, **4d**, and **4j** are shown in Figures S1–S3, respectively. The selected bond lengths and bond angles are summarized in Table 3. Just like complex **4u** reported previously,<sup>17b</sup> in the solid state, these complexes all adopt distorted octahedral geometry around the titanium center. For complexes **4a–d** and **4j**, the two oxygen atoms are situated in *trans* position, while the two nitrogen atoms are in *cis* position to each other, and so are the two chlorine atoms around the central titanium metal. However, for complex **4m**, the two oxygen atoms, the two nitrogen atoms, and the two chlorine atoms are all in *trans* position (Cl–Ti–Cl angle,  $180.0^{\circ}$ ; N–Ti–N angle,  $180.00(10)^{\circ}$ ; O–Ti–O angle,  $180.0^{\circ}$ ) around the central titanium metal.

The Ti–Cl bond distances for complexes **4b** (2.2793 Å), **4c** (2.2755 Å), and **4d** (2.2712 Å) are close to that of complex **4a** (2.2787 Å), but obviously longer than that of complex **4j** (2.2623 Å). Complexes **4b** (Cl–Ti–Cl,  $98.09^{\circ}$ ), **4c** (Cl–Ti–Cl,  $99.85^{\circ}$ ), and **4d** (Cl–Ti–Cl,  $100.04^{\circ}$ ) show narrower Cl–Ti–Cl angles compared with complex **4a** (Cl–Ti–Cl,  $100.76^{\circ}$ ), while complex **4j** (Cl–Ti–Cl,  $100.35^{\circ}$ ) exhibits Cl–Ti–Cl angles similar to complex **4a**. These differences in bond length and angles probably originate from the steric hindrance and electronic effects caused by fluorine atom(s) introduced.

Interestingly, the X-ray diffraction of a single crystal displays two different signals (F5 and F5') in the ratio of 6:4 for complex **4b**, which has only one fluorine atom adjacent to each imine group, suggesting that two or more isomers of **4b** exist in the solid state. In our previous work,<sup>17</sup> the  $^1\text{H}$  NMR spectra of titanium complexes **4a** and **4u** displayed a single sharp resonance for the methine proton ( $-\text{CH}=\text{C}-$ ) of the  $\beta$ -enaminoketonato chelate ligands in accordance with only one isomer of octahedral coordination structure. Complexes **4d**, **4h**, **4j**, **4l**, and **4o–t** are similar to **4a** and **4u**, with only a single sharp resonance for the methine proton, respectively. By contrast, for complexes **4b**, **4c**, **4e–g**, **4i**, **4k**, and **4n**, of which the two  $\beta$ -enaminoketonato ligands bear asymmetric N-phenyl rings, the  $^1\text{H}$  NMR and  $^{19}\text{F}$  NMR data in  $\text{CDCl}_3$  solution at  $25\text{ }^{\circ}\text{C}$  suggest that there are not less than two isomers. For example, the  $^1\text{H}$  NMR spectrum ( $\text{CDCl}_3$ , 300 MHz) of complex **4b** shows four resonances (6.09, 6.02, 5.98, 5.87 ppm) in the ratio 10:4:2:11 for the two methine protons of the ligands, and in  $o\text{-C}_6\text{D}_4\text{Cl}_2$  there are even five different resonances for the same protons. In

the  $^{19}\text{F}$  NMR spectra of **4b**, there are also four resonances ( $-115.5$ ,  $-117.9$ ,  $-118.4$ ,  $-121.1$  ppm) in the ratio 14:6:15:2 for the two fluorine atoms on N-aryl moieties of the ligands. The number of signals, which is more than the previous results, revealed that there are not less than two isomers in the solution, because one isomer shows not more than two signals in the  $^1\text{H}$  NMR for two methine protons and in the  $^{19}\text{F}$  NMR for two fluorine atoms on the imine phenyl ring. A variable-temperature  $^1\text{H}$  NMR experiment in the range  $20\text{--}150\text{ }^{\circ}\text{C}$  revealed a trend of gradual coalescence of the signals of the isomers with an increase in temperature (Figure 4). These data were consistent with a rotational barrier to interconversion of the isomers of **4b**. Due to the rotation of the N1–C15 and N2–C1 bonds, complex **4b** possibly exists as three relatively stable conformational isomers (Scheme 3), with RFE values of 4.915 kJ/mol (**I**), 0 kJ/mol (**II**), and 3.341 kJ/mol (**III**), respectively, according to DFT calculation. On the basis of the RFE values, the ratio of the three conformational isomers was calculated to be 0.26:1.0:0.14 by the Boltzman distribution.<sup>19</sup> The most abundant isomer is thought to be the lowest energy conformational isomer (**II**), in which one fluorine atom of the N-aryl is oriented to the chlorine atom and the other fluorine atom of the N-aryl is away from the chlorine atom. This supposition can be confirmed by the  $^1\text{H}$  NMR spectra: the two methine protons of asymmetric conformational isomer **II** show two different signals, while the two methine protons of symmetric conformational isomers **I** and **III** show only one signal, and the ratio of the methine protons almost accords with the ratio of the three conformational isomers calculated.

The RFE values of the three isomers of the other complexes are also calculated by DFT and summarized in Table 4. The data indicate that the most stable conformational isomer is **II** for the complexes bearing an *ortho*-fluorine atom on each N-aryl ring, while for those complexes with a *meta*-fluorine atom or trifluoromethyl group but not an *ortho*-fluorine atom, the most stable conformational isomer is **III**. The H–H COSY spectra (Figure 5) also confirm that complex **4c** displays three conformational isomers. These spectra show clearly four unrelated resonances (5.8–6.2 ppm) for the methine protons of the ligands. A similar phenomenon of two rotational isomers was observed in  $t\text{-Bu}_2(2\text{-C}_6\text{H}_4\text{Ph})\text{PNTi}(\text{CH}_2\text{Ph})_3$  by Stephan and his co-workers<sup>20a,b</sup> and in the heteroligated (salicylaldiminato)( $\beta$ -enaminoketonato) titanium complexes reported by Lancaster's group.<sup>20c</sup>

**Ethylene Polymerization.** With MMAO as a cocatalyst, new titanium complexes **4b–r**, bearing EWG on their ligands, have been investigated as effective catalysts for ethylene polymerization at room temperature under atmospheric pressure. The results are summarized in Table 5. The data demonstrate that the introduction of EWG onto the N-aryl moiety significantly affects catalytic activity and the properties of the resultant polymers. The melting temperatures of the resultant polyethylene are between  $135$  and  $140\text{ }^{\circ}\text{C}$ , suggesting the resultant polymers are linear polyethylene. Furthermore, the linear structure of the polyethylenes was also proved by  $^{13}\text{C}$  NMR analysis.

(18) (a) Tang, L. M.; Duan, Y. Q.; Li, Y. S. *J. Polym. Sci. Part A: Polym. Chem.* **2005**, *43*, 1681. (b) Tang, L. M.; Hu., T.; Pan., L.; Li, Y. S. *J. Polym. Sci. Part A: Polym. Chem.* **2005**, *43*, 6323.

(19) According to the Boltzman distribution, the ratio of the conformational isomers based on the relative energy of the isomers,  $N_{\text{I}}:N_{\text{II}}:N_{\text{III}} = e^{-\Delta E_{\text{I}}/RT}:e^{-\Delta E_{\text{II}}/RT}:e^{-\Delta E_{\text{III}}/RT}$ . Atkins, P. W., Ed. *Physical Chemistry*; Oxford University Press: London, 1978; pp 12, 659 ff.

Table 1. Relative Formation Energies (RFE) of the Five Different Configuration Isomers of Some Representative Titanium Complexes (kJ/mol)

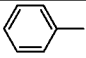
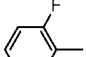
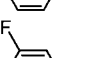
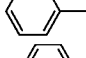
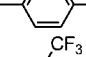
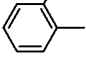
Code	Aryl structure	<i>cis</i> -I	<i>cis</i> -II	<i>cis</i> -III	<i>trans</i> -I	<i>trans</i> -II
4a		0	18.4	20.9	237.2	13.5
4b		0	18.3	15.1	241.3	14.2
4c		0	19.7	23.5	247.1	16.7
4d		0	16.3	20.0	253.0	13.0
4m		50.5	27.4	7.68	310.2	0
4n		0	17.8	20.7	267.2	13.8

Table 2. Crystal Data and Structure Refinements of Complexes 4a–d, 4j, and 4m

	4a	4b	4c	4d	4j	4m
empirical formula	C <sub>28</sub> H <sub>30</sub> Cl <sub>2</sub> F <sub>6</sub> N <sub>2</sub> O <sub>2</sub> Ti	C <sub>28</sub> H <sub>28</sub> Cl <sub>2</sub> F <sub>8</sub> N <sub>2</sub> O <sub>2</sub> Ti	C <sub>28</sub> H <sub>28</sub> Cl <sub>2</sub> F <sub>8</sub> N <sub>2</sub> O <sub>2</sub> Ti	C <sub>28</sub> H <sub>26</sub> Cl <sub>2</sub> F <sub>8</sub> N <sub>2</sub> O <sub>2</sub> Ti	C <sub>28</sub> H <sub>26</sub> Cl <sub>2</sub> F <sub>10</sub> N <sub>2</sub> O <sub>2</sub> Ti	C <sub>30</sub> H <sub>28</sub> Cl <sub>2</sub> F <sub>12</sub> N <sub>2</sub> O <sub>2</sub> Ti
fw	659.34	695.32	695.32	695.32	731.33	795.34
crystal system	orthorhombic	tetragonal	monoclinic	monoclinic	monoclinic	monoclinic
space group	<i>Pbca</i>	<i>P4<sub>2</sub>/n</i>	<i>C2/c</i>	<i>P2<sub>1</sub>/n</i>	<i>P2<sub>1</sub>/n</i>	<i>P2<sub>1</sub>/c</i>
<i>a</i> (Å)	19.2495(11)	25.7113(7)	12.840(2)	8.5961(5)	13.9050(8)	9.6966(9)
<i>b</i> (Å)	16.5177(9)	25.7113(7)	15.936(2)	35.172(2)	16.9870(10)	8.6009(8)
<i>c</i> (Å)	19.7412(11)	9.8977(6)	15.369(2)	10.6131(6)	15.1935(9)	20.8763(19)
$\beta$ (deg)	90	90	94.637(2)	102.4990(10)	99.9150(10)	102.9830(10)
<i>V</i> (Å <sup>3</sup> ), <i>Z</i>	6276.9(6)	6543.1(5), 8	3134.4(8), 4	3132.7(3), 4	3535.2(4), 4	1696.6(3), 2
density (Mg/m <sup>3</sup> )	1.395	1.408	1.473	1.474	1.415	1.557
absorp coeff (mm <sup>-1</sup> )	0.506	0.498	0.520	0.520	0.474	0.507
<i>F</i> (000)	2704	2816	1416	1416	1530	804
cryst size (mm)	0.44 × 0.39 × 0.16	0.48 × 0.28 × 0.10	0.41 × 0.14 × 0.11	0.36 × 0.23 × 0.12	0.43 × 0.13 × 0.07	0.39 × 0.16 × 0.06
$\theta$ range for data collection (deg)	1.92 to 26.02	1.58 to 26.04	2.04 to 25.34	2.05 to 26.05	1.83 to 26.04	2.00 to 26.02
no. of refls collected	33 618	35 598	7986	17 525	20 253	9112
no. of indep refls	6179 ( <i>R</i> <sub>int</sub> = 0.0291)	6445 ( <i>R</i> <sub>int</sub> = 0.0327)	2877 ( <i>R</i> <sub>int</sub> = 0.0379)	6162 ( <i>R</i> <sub>int</sub> = 0.0260)	6954 ( <i>R</i> <sub>int</sub> = 0.0366)	3322 ( <i>R</i> <sub>int</sub> = 0.0324)
absorption correction			semiempirical from equivalents			
max. and min. transmittance	0.9239 and 0.8065	0.9510 and 0.7954	0.9441 and 0.8164	0.9426 and 0.8345	0.9698 and 0.8213	0.9688 and 0.8252
no. of data/restraints/params	6179/2/406	6445/6/412	2877/0/ 198	6162/36/ 378	6954/2/440	3322/ 0/226
goodness-of-fit on <i>F</i> <sup>2</sup>	1.021	1.138	1.109	1.011	0.968	1.016
final <i>R</i> indices [ <i>I</i> > 2 $\sigma$ ( <i>I</i> )]: <i>R</i> <sub>1</sub> , <i>wR</i> <sub>2</sub>	0.0400, 0.1056	0.0560, 0.1833	0.0632, 0.1390	0.0681, 0.1965	0.0507, 0.1622	0.0448, 0.1017
largest diff peak and hole (e Å <sup>-3</sup> )	0.425 and -0.354	1.618 and -0.256	0.897 and -0.362	1.371 and -0.573	0.957 and -0.276	0.486 and -0.234

Introduction of electron-withdrawing fluorine atoms into a  $\beta$ -enaminoketonato ligand will decrease the electron density on "N" coordinated to the metal titanium, which will decrease the electron density of the center titanium. Accordingly, it will make ethylene coordinate to the center titanium much easier and enhance catalytic activity. As a result, fluorinated complexes **4b–d**, with one fluorine atom on the each N-aryl moiety, all display much higher activities toward ethylene polymerization (8.40, 9.24, and 9.60 kg PE/mmol<sub>Ti</sub>·h, respectively) than complex **4a** (4.32 kg PE/mmol<sub>Ti</sub>·h). Although the electronic effect of an *ortho*-fluorine atom is similar to that of a *para* one,<sup>22</sup> complex **4b**, in which the N-aryl moiety bears one *ortho*-fluorine atom, displays lower

activity than that of **4d**, with one fluorine atom at the *para*-position on its N-aryl moiety. One probable reason is that the steric effect of *ortho*-fluorine atoms of an N-aryl moiety of the ligand hinders ethylene access to the center titanium, leading to a decreased rate of ethylene polymerization.

The data listed in Table 5 also indicate that the polyethylenes obtained from complexes **4b–d** all display high molecular weights like that obtained from complex **4a**. It is noteworthy that a relatively narrow molecular weight distribution (PDI = 1.5) of the polymer produced by complex **4b** was observed (entry 2), although it displays more than one conformational isomer in solution. This result indicates that the active centers of complex **4b** from different conformational isomers are identical or very similar to each other. In order to further clarify this point, we studied the active intermediates in ethylene polymerization of complex **4b** by <sup>1</sup>H NMR spectroscopy. It is well known that the process of

(20) (a) Ghesner, I.; Fenwick, A.; Stephan, D. W. *Organometallics* **2006**, *25*, 4985–4995. (b) Graham, T. W.; Kickham, J.; Courtenay, S.; Wei, P.; Stephan, D. W. *Organometallics* **2004**, *23*, 3309. (c) Pennington, D. A.; Harrington, R. W.; Clegg, W.; Bochmann, M.; Lancaster, S. J. *J. Organomet. Chem.* **2006**, *691*, 3183.

(21) Vanka, K.; Xu, Z.; Ziegler, T. *Organometallics* **2004**, *23*, 2900–2910.

(22) Morison, R. T., Boyd R. M., Ed. *Organic Chemistry*, 4th ed.; Allyn and Bacon, Inc.: Boston, 1983; pp 614–620.

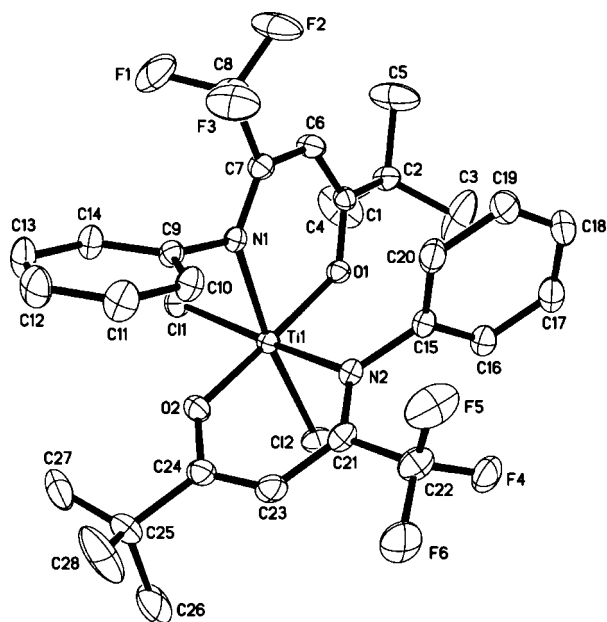


**Figure 1.** Molecular structure of complex **4a** with thermal ellipsoids at the 30% probability level. Hydrogen atoms are omitted for clarity.

the activation of titanium complexes by MMAO includes two steps: first, the alkylation of the precatalyst, and second, the cationation of the alkyl complex.<sup>23</sup> By mixing precatalyst **4b** and dried MMAO, we found that the conformational isomerization of the precatalyst and the cationic alkyl complex generated on catalyst activation was very different. As shown in Figure 6, when the Al/Ti molar ratio was about 25, the signal of an alkyl complex was generated ( $\delta = 5.83$  ppm). If the Al/Ti molar ratio increased to 50, the signal of the precatalyst (5.96–6.16) almost disappeared. It is clearly observed that the methine proton ( $-\text{CH}=\text{C}-$ ) of the  $\beta$ -enaminoketonato chelate ligands in the alkyl complex displays only a single sharp signal, which means the alkyl complex or the cation exists as only one conformation, while the dichlorides **4b** have three conformational isomers.

Interestingly, with two fluorine atoms on the N-aryl moiety of the ligand, complexes **4e–j** show more complicated catalytic behavior compared with **4b–d**. Among these catalysts, complexes **4e–g** and **4i** show similar catalytic activities toward ethylene polymerization (7.44, 7.20, 7.80, and 7.08 kg PE/mmol<sub>Ti</sub>·h, respectively), which are much higher than **4a** (4.32 kg PE/mmol<sub>Ti</sub>·h), but lower than **4b–d**, and complex **4j** displays somewhat lower catalytic activity (4.08 kg PE/mmol<sub>Ti</sub>·h) than **4a**, while complex **4h** exhibits much lower catalytic activity (1.56 kg PE/mmol<sub>Ti</sub>·h) than **4a**.

Compared with complex **4b** or **4d**, complexes **4e–g** and **4i**, which bear two fluorine atoms on each ligand, show similar catalytic activities due to the similar electronic effect. Obviously, the titanium center of complex **4h** is more crowded than those of complexes **4e–g**, which hinders the coordination of ethylene and considerably decreases catalytic activity toward ethylene polymerization. Due to the stronger inductive effect of four

*meta*-fluorine atoms,<sup>22</sup> the titanium center of complex **4j** is more strongly electrophilic than complexes **4e–g** and **4i**, which will considerably slow the ethylene migration to the metal carbon bond and decrease catalytic activity.

It is significant to note that the polyethylenes produced by complexes **4e–h**, similar to complex **4b**, with fluorine atom(s) adjacent to the imine nitrogen also display narrower molecular weight distributions (entries 5–8, PDI = 1.5–1.6). Alternatively, broader molecular weight distributions of the polyethylenes yielded by other complexes with no fluorine adjacent to the imine nitrogen are comparable to the values yielded by complex **4a** (entry 1, PDI = 1.8). These results clearly indicate that the presence of a fluorine atom adjacent to the imine nitrogen in the ligand accelerates the chain propagation and decelerates the chain transfer. Perhaps the *ortho*-fluorine atoms provide a compact transition state that assists chain propagation.<sup>24</sup> These results are similar to those of the phenoxyimine titanium catalysts studied by Fujita and Coates.<sup>14c,24</sup>

By introducing an extra fluorine atom to complex **4i**, we obtained complexes **4k** and **4l**, which show lower activities (4.80 and 2.76 kg PE/mmol<sub>Ti</sub>·h, respectively) than **4i** (7.08 kg PE/mmol<sub>Ti</sub>·h). The low activities of **4k** and **4l** may be attributed to their stronger electrophilic titanium centers and the lower stability of the catalytic species originating from the strong electron-withdrawing effect. These results indicate that the catalytic activity decrease with further increase of the fluorine atoms on N-aryl ring in general.

We also explored the effect of reaction parameters such as ethylene pressure, catalyst concentration, and reaction time on the ethylene polymerization behavior of some selected fluorinated complexes. The typical polymerization results are summarized in Table 6. Compared with the results obtained at atmospheric pressure, larger differences at 4 atm ethylene pressure in catalytic activities were observed while the catalytic activity decreased in the same order: **4d** > **4c** > **4b**, **4f** > **4k**, **4j** (entries 2, 4, 11–14). The observed catalytic activities changed only slightly if **4b** was used, whereas that of **4k** shows larger changes at various catalyst concentrations (entries 5–10). Both analogues exhibited rather high catalytic activity for at least 15 min (entries 15–18). For both **4b** and **4k**, the effect of ethylene pressure on catalytic activity was nonlinear (entries 1–4).

With other EWGs introduced to the  $\beta$ -enaminoketonato ligands, similar results were observed. For example, aromatic-chlorine/iodine-substituted complexes **4p** and **4q** also display much higher catalytic activities (8.16 and 7.56 kg PE/mmol<sub>Ti</sub>·h, respectively) than unsubstituted complex **4a**, but lower than the corresponding aromatic-fluorine-substituted complex **4d**. This order of the catalytic activities indicates that the fluorine atom can enhance the catalytic activity more effectively than other halogen substituents. Interestingly, complex **4o**, with a trifluoromethyl group as a nonconjugated electron-withdrawing group in *para*-position, also shows much higher activity (7.08 kg PE/mmol<sub>Ti</sub>·h) compared with complex **4a**. However, complex **4m**, with an *ortho*-trifluoromethyl group does not exhibit any catalytic activity due to the *trans*-configuration of the two chlorine atoms. In addition, complex **4r**, bearing strongly electron-withdrawing *para*-nitro substituents, on the N-aryl moieties of the ligands, displays much lower catalytic activity (1.20 kg PE/mmol<sub>Ti</sub>·h) than its mother complex **4a**.

(23) (a) Makio, H.; Fujita, T. *Macromol. Symp.* **2004**, *213*, 221–233. (b) Bryliakov, K. P.; Kravtsov, E. A.; Pennington, D. A.; Lancaster, S. J.; Bochmann, M.; Brintzinger, H. H.; Talsi, E. P. *Organometallics* **2005**, *24*, 5660–5664. (c) Volkis, V.; Rodensky, M.; Lisovskii, A.; Balazs, Y.; Eisen, M. S. *Organometallics* **2006**, *25*, 4934–4937. (d) Gornshtein, F.; Kapon, M.; Botoshansky, M.; Eisen, M. S. *Organometallics* **2007**, *26*, 497–507.

(24) (a) Talarico, G.; Busico, V.; Cavallo, L. *Organometallics* **2004**, *23*, 5989–5993. (b) Busico, V.; Talarico, G.; Cipullo, R. *Macromol. Symp.* **2005**, *226*, 1–16.

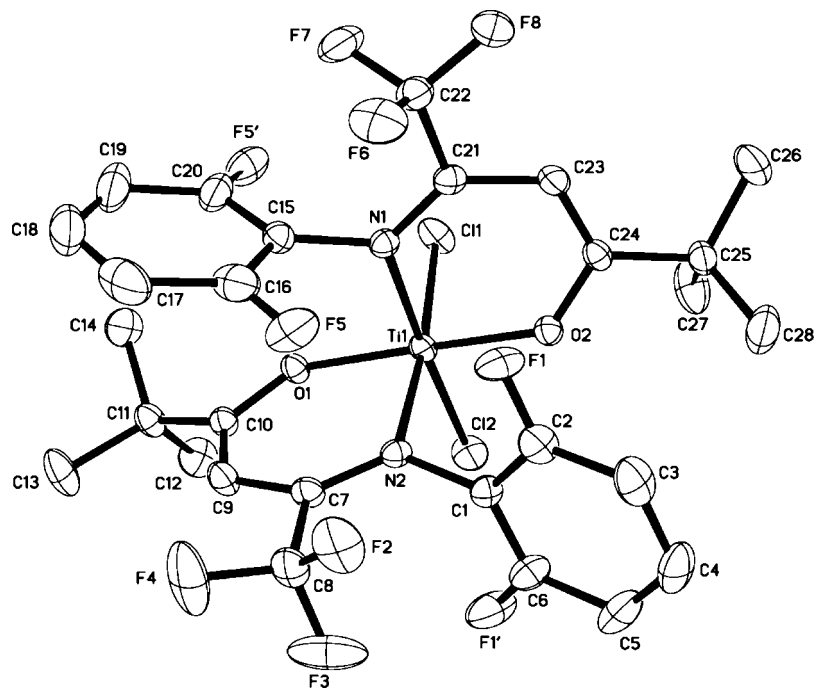


**Figure 2.** Molecular structure of complex **4b**. Occupancy factors for F5 and F5' are 0.6 and 0.4, respectively, with thermal ellipsoids at the 30% probability level. Hydrogen atoms are omitted for clarity.

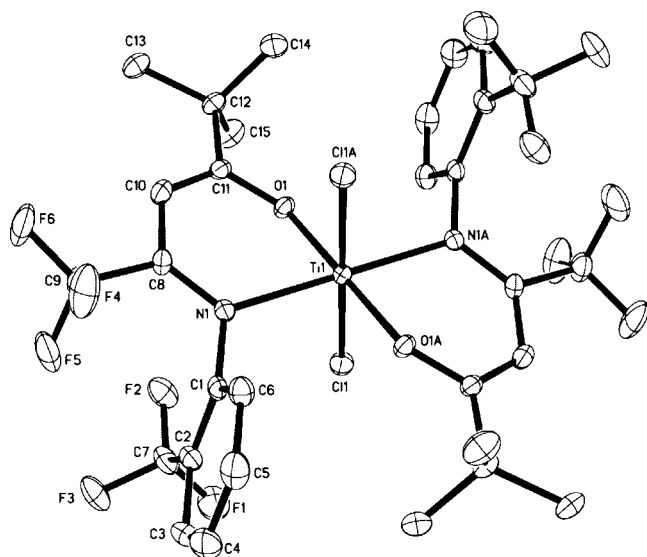


**Figure 3.** Molecular structure of complex **4m** with thermal ellipsoids at the 30% probability level. Hydrogen atoms are omitted for clarity.

Perhaps, in this case, the catalytic species is less stable, and some deactivation reaction takes place.

In order to study the effect of  $\beta$ -enaminoketonato ligand conjugacy on the catalytic activity of the titanium complex, we synthesized complexes **4s** and **4t** without a conjugated phenyl. The two complexes show only extremely low activities (0.036 and 0.048 kg PE/mmol<sub>Ti</sub>·h), which clearly indicates that a conjugated system is essential for the polymerization in this system.

### Conclusions

A series of novel titanium complexes (**4b–t**) bearing two  $\beta$ -enaminoketonato ligands with or without electron-withdrawing group(s) have been synthesized and characterized. In the solid

state, these complexes all adopt distorted octahedral geometry around the titanium center. For all the complexes except for **4m**, the two chlorine atoms are in a *cis*-position to each other. However, for complex **4m**, with a bulky CF<sub>3</sub> in the *ortho*-position of each N-aryl ring, the two chlorine atoms are in a *trans*-position around the central titanium metal. In addition, the complexes bearing two ligands of which the N-aryl is asymmetrical, such as **4b**, display not less than two conformational isomers in both the solid state and solution. With MMAO as a cocatalyst, most titanium complexes are efficient precatalysts for ethylene polymerization. Catalytic activity and polymer property are influenced significantly by the structure of the  $\beta$ -enaminoketonato ligand. Both electronic effects (including conjugative and inductive effects) and steric effects of the ligand considerably influence the ethylene polymerization behavior of the titanium complexes. Introduction of one fluorine atom, an electron-withdrawing group, into each N-aryl ring causes an enhancement in catalytic activity by about 100%. However, further introducing fluorine atoms into the ligands results in a decrease in catalytic activity. The presence of a fluorine atom adjacent to the imine nitrogen in the ligand suppresses  $\beta$ -hydrogen transfer to some extent, like the case of FI catalysts. Introducing a bulky substituent, even with a strong EWG, into the *ortho*-position of the imine group of the ligands results in the *trans*-configuration of the two chlorine atoms of the titanium complex, and such a complex will be inactive toward ethylene polymerization. Furthermore, the titanium complex displays only low catalytic activity for ethylene polymerization if there is no conjugation between the  $\beta$ -enaminoketonato and the substituent linking the imine group.

### Experimental Section

**General Procedures and Materials.** All air- and moisture-sensitive compounds were manipulated using standard Schlenk techniques or in a glovebox under an argon atmosphere. NMR data of the ligands and the complexes were obtained on a Bruker 300 MHz spectrometer at ambient temperature with CDCl<sub>3</sub> as a solvent (dried by MS 4 Å). The <sup>19</sup>F NMR data of the complexes were

**Table 3.** Selected Bond Lengths (Å) and Angles (deg) for Complexes **4a–d**, **4j**, and **4m**

	<b>4a</b>	<b>4b</b>	<b>4c</b>	<b>4d</b>	<b>4j</b>	<b>4m</b>
Bond Distances						
Ti–O (1)	1.8748(14)	1.865 (2)	1.878(2)	1.884(3)	1.890 (2)	1.9006(15)
Ti–O (2)	1.9000(14)	1.886 (2)	1.878(2)	1.879(3)	1.8737 (19)	1.9006(15)
Ti–N (1)	2.2025(16)	2.215(3)	2.197(3)	2.207(3)	2.183(2)	2.1736(19)
Ti–N (2)	2.1891(17)	2.210 (3)	2.197(3)	2.197(3)	2.235 (2)	2.1736(19)
Ti–Cl (1)	2.2844(6)	2.2767 (11)	2.2755(11)	2.2761(12)	2.2637 (8)	2.2926(6)
Ti–Cl (2)	2.2729(6)	2.2819 (10)	2.2755(11)	2.2663(12)	2.2608 (9)	2.2926(6)
Bond Angles						
N (1)–Ti–N (2)	83.89 (6)	85.61 (10)	84.02 (15)	83.91(12)	83.17 (8)	180.00(10)
O (1)–Ti–O (2)	170.35 (7)	167.17 (10)	169.11 (16)	168.60(13)	170.48 (9)	180.0
Cl (1)–Ti–Cl (2)	100.76 (3)	98.09 (4)	99.85 (8)	100.04(5)	100.35 (3)	180.0
N (1)–Ti–O (1)	82.33 (6)	90.60 (10)	82.29 (11)	89.42 (12)	81.53 (8)	83.61(7)
N (1)–Ti–O (2)	89.92 (6)	81.31 (10)	89.61 (11)	81.53 (12)	91.19 (8)	96.39(7)
N (1)–Ti–Cl (1)	87.20 (5)	86.41 (8)	88.16 (8)	88.73(8)	91.25 (6)	93.18(5)

obtained with fluorobenzene as internal standard ( $\delta_F = -112.6$  ppm).<sup>25</sup> The variable-temperature <sup>1</sup>H NMR data of complex **4b** were obtained on a Varian Unity-400 MHz spectrometer from 293 to 423 K with *o*-C<sub>6</sub>D<sub>4</sub>Cl<sub>2</sub> as a solvent. Elemental analyses were performed on a Perkin-Elmer Series II CHN/O analyzer 2400. DSC measurements were performed on a Perkin-Elmer Pyris 1 differential scanning calorimeter. Melting temperatures were recorded in the second heating run at a heating rate of 10 °C/min. The number-average molecular weights ( $\bar{M}_n$ ) and polydispersity indexes (PDI) of the polymers obtained were determined in 1,2,4-trichlorobenzene at 150 °C on a high-temperature GPC using a PL-GPC 220 instrument equipped with three PLgel 10 μm mixed-B LS columns.<sup>17</sup>

Dried diethyl ether, hexane, and toluene were purified by an M. Braun solvent purification system (SPS). 1,1,1-Trifluoro-5,5-dimethyl-2,4-hexanedione was synthesized according to the literature.<sup>26</sup> Aniline derivatives for ligand synthesis were purchased from Aldrich Chemical or Acros Organics and used without further purification. Commercial titanium tetrachloride was distilled prior

to use. The 1.6 M *n*-butyllithium solution in hexane was purchased from Acros. Modified methylaluminoxane (MMAO, 7% aluminum in heptane solution) was purchased from Akzo Nobel Chemical Inc. Dried MMAO was prepared from commercial MMAO by removal of the solvent in vacuo at 50 °C. Commercial ethylene was directly used for polymerization without further purification. Complexes **4a** and **4u** were synthesized according to the procedure reported previously.<sup>17b</sup>

**Synthesis of Ligands 2b–t.** *o*-FPhN=C(CF<sub>3</sub>)CHC(*t*-Bu)OH (**2b**). To a stirred solution of 1,1,1-trifluoro-5,5-dimethyl-2,4-hexanedione (4.9 g, 25 mmol) in dried toluene (50 mL) were added 2-fluoroaniline (2.22 g, 20 mmol) and *p*-toluenesulfonic acid (ca. 20 mg) as a catalyst at room temperature. The mixture was heated and refluxed, and the water formed was removed azeotropically using a Dean-Stark apparatus for 24 h. During the stirring period, a light yellow solution was formed. Evaporation of toluene gave a deep yellow oil. The crude product was purified by column chromatography on silica gel with petroleum ether–ethyl acetate (200:1) as an eluent, affording **2b** (3.37 g, 11.7 mmol) as a light yellow oil in 58% yield. <sup>1</sup>H NMR (CDCl<sub>3</sub>): δ 11.46 (s, 1H, O-H), 7.21–7.02 (m, 4H, Ph-H), 5.90 (s, 1H, =CH), 1.14 (s, 9H, *t*-Bu). <sup>13</sup>C NMR (CDCl<sub>3</sub>): δ 206.82, 156.61, 146.60, 127.56, 127.45, 124.91, 123.10, 118.97, 114.88, 91.08, 42.04, 25.93. Anal. Calcd for C<sub>14</sub>H<sub>15</sub>F<sub>4</sub>NO: C, 58.13; H, 5.23; N, 4.84. Found: C, 58.00; H, 5.19; N, 4.80.

*m*-FPhN=C(CF<sub>3</sub>)CHC(*t*-Bu)OH (**2c**). Compound **2c** was prepared via a procedure similar to that for **2b** as a light yellow oil in 69% yield. <sup>1</sup>H NMR (CDCl<sub>3</sub>): δ 11.75 (s, 1H, O-H), 7.15–6.81 (m, 4H, Ph-H), 5.87 (s, 1H, =CH), 1.13 (s, 9H, *t*-Bu). <sup>13</sup>C NMR (CDCl<sub>3</sub>): δ 208.22, 163.09, 147.23, 140.10, 130.43, 121.55, 120.53, 113.87, 113.20, 92.42, 43.38, 27.29. Anal. Calcd for C<sub>14</sub>H<sub>15</sub>F<sub>4</sub>NO: C, 58.13; H, 5.23; N, 4.84. Found: C, 58.31; H, 5.27; N, 4.79.

*p*-FPhN=C(CF<sub>3</sub>)CHC(*t*-Bu)OH (**2d**). Compound **2d** was prepared via a procedure similar to that for **2b** as a light yellow solid in 75% yield. <sup>1</sup>H NMR (CDCl<sub>3</sub>): δ 11.65 (s, 1H, O-H), 7.13–6.69 (m, 4H, Ar), 5.84 (s, 1H, =CH), 1.18 (s, 9H, *t*-Bu). <sup>13</sup>C NMR (CDCl<sub>3</sub>): δ 206.74, 160.44, 146.83, 132.94, 127.14, 119.19, 114.73, 90.03, 41.94, 26.03. Anal. Calcd for C<sub>14</sub>H<sub>15</sub>F<sub>4</sub>NO: C, 58.13; H, 5.23; N, 4.84. Found: C, 58.24; H, 5.20; N, 4.86.

2,3-F<sub>2</sub>PhN=C(CF<sub>3</sub>)CHC(*t*-Bu)OH (**2e**). Compound **2e** was prepared via a procedure similar to that for **2b** as a light yellow oil in 71% yield. <sup>1</sup>H NMR (CDCl<sub>3</sub>): δ 11.73 (s, 1H, O-H), 7.14–6.96 (m, 3H, Ar), 6.02 (s, 1H, =CH), 1.23 (s, 9H, *t*-Bu). <sup>13</sup>C NMR (CDCl<sub>3</sub>): δ 207.88, 150.69, 146.19, 147.14, 128.02,

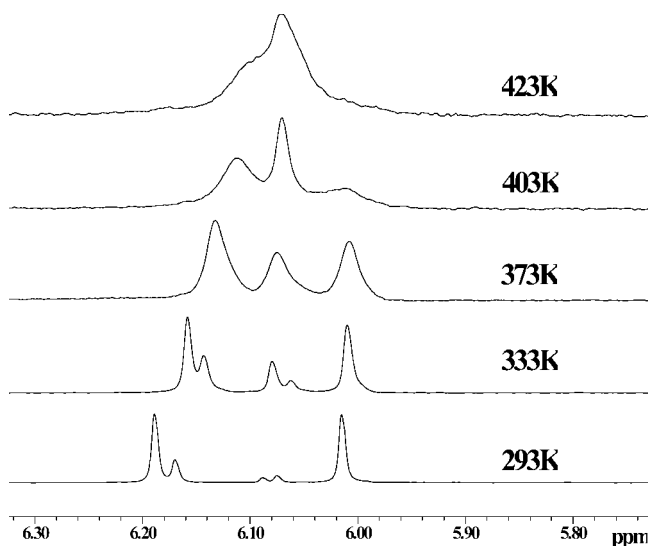
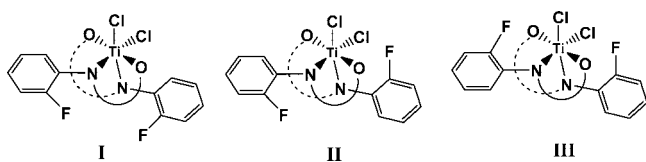


**Figure 4.** Variable-temperature <sup>1</sup>H NMR spectra of **4b** in *o*-C<sub>6</sub>D<sub>4</sub>Cl<sub>2</sub>.

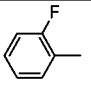
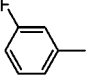
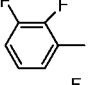
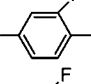
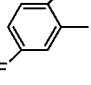
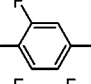
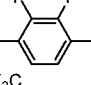
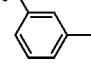
**Scheme 3.** Structures of Three Conformational Isomers of Complex **4b**



(25) Davis, F. A.; Han, W.; Murphy, C. K. *J. Org. Chem.* **1995**, *60*, 4730.

(26) Schlesinger, H. I.; Brown, H. C.; Katz, J. J.; Archer, S.; Lad, R. A. *J. Am. Chem. Soc.* **1953**, *75*, 2446.

Table 4. Relative Formation Energies (RFE) of the Three Different Conformational Isomers of Some Titanium Complexes (kJ/mol)

code	aryl structure	isomer I	isomer II	isomer III
4b		3.34	0	4.92
4c		2.11	0.85	0
4e		1.43	0	3.98
4f		2.38	0	5.31
4g		4.61	0	6.41
4i		2.31	0.62	0
4k		0.24	0	4.19
4n		0.86	0.30	0

123.23, 119.98, 115.64, 114.46, 92.91, 43.02, 26.62. Anal. Calcd for  $C_{14}H_{14}F_5NO$ : C, 54.73; H, 4.59; N, 4.56. Found: C, 54.59; H, 4.55; N, 4.52.

**2,4-F<sub>2</sub>PhN=C(CF<sub>3</sub>)CHC(*t*-Bu)OH (2f).** Compound **2f** was prepared via a procedure similar to that for **2b** as a light yellow oil in 61% yield. <sup>1</sup>H NMR (CDCl<sub>3</sub>):  $\delta$  11.27 (s, 1H, O-H), 7.22–6.76 (m, 3H, Ar), 5.84 (s, 1H, =CH), 1.15 (s, 9H, *t*-Bu). <sup>13</sup>C NMR (CDCl<sub>3</sub>):  $\delta$  207.00, 160.72, 157.31, 146.89, 129.25, 119.04, 121.08, 110.30, 103.42, 91.14, 42.12, 25.91. Anal. Calcd for  $C_{14}H_{14}F_5NO$ : C, 54.73; H, 4.59; N, 4.56. Found: C, 54.67;

H, 4.63; N, 4.53.

**2,5-F<sub>2</sub>PhN=C(CF<sub>3</sub>)CHC(*t*-Bu)OH (2g).** Compound **2g** was prepared via a procedure similar to that for **2b** as a light yellow oil in 74% yield. <sup>1</sup>H NMR (CDCl<sub>3</sub>):  $\delta$  11.58 (s, 1H, O-H), 7.26–6.90 (m, 3H, Ar), 6.02 (s, 1H, =CH), 1.22 (s, 9H, *t*-Bu). <sup>13</sup>C NMR (CDCl<sub>3</sub>):  $\delta$  207.00, 157.17, 152.46, 145.54, 126.13, 119.11, 115.47, 113.16, 113.06, 92.35, 42.20, 25.79. Anal. Calcd for  $C_{14}H_{14}F_5NO$ : C, 54.73; H, 4.59; N, 4.56. Found: C, 54.86; H, 4.54; N, 4.59.

**2,6-F<sub>2</sub>PhN=C(CF<sub>3</sub>)CHC(*t*-Bu)OH (2h).** Compound **2h** was prepared via a procedure similar to that for **2b** as a deep yellow oil in 64% yield. <sup>1</sup>H NMR (CDCl<sub>3</sub>):  $\delta$  11.03 (s, 1H, O-H), 7.30–6.91 (m, 3H, Ar), 6.02 (s, 1H, =CH), 1.23 (s, 9H, *t*-Bu). <sup>13</sup>C NMR (CDCl<sub>3</sub>):  $\delta$  207.12, 158.86, 147.39, 128.22, 118.87, 114.30, 110.51, 91.59, 42.17, 25.82. Anal. Calcd for  $C_{14}H_{14}F_5NO$ : C, 54.73; H, 4.59; N, 4.56. Found: C, 54.66; H, 4.63; N, 4.59.

**3,4-F<sub>2</sub>PhN=C(CF<sub>3</sub>)CHC(*t*-Bu)OH (2i).** Compound **2i** was prepared via a procedure similar to that for **2b** as a deep yellow solid in 72% yield. <sup>1</sup>H NMR (CDCl<sub>3</sub>):  $\delta$  11.73 (s, 1H, O-H), 7.17–6.93 (m, 3H, Ar), 5.88 (s, 1H, =CH), 1.22 (s, 9H, *t*-Bu). <sup>13</sup>C NMR (CDCl<sub>3</sub>):  $\delta$  207.77, 150.01, 149.27, 147.90, 134.38, 122.32, 120.04, 117.06, 115.53, 91.81, 42.89, 26.68. Anal. Calcd for  $C_{14}H_{14}F_5NO$ : C, 54.73; H, 4.59; N, 4.56. Found: C, 54.57; H, 4.55; N, 4.53.

**3,5-F<sub>2</sub>PhN=C(CF<sub>3</sub>)CHC(*t*-Bu)OH (2j).** Compound **2j** was prepared via a procedure similar to that for **2b** as a light yellow oil in 80% yield. <sup>1</sup>H NMR (CDCl<sub>3</sub>):  $\delta$  11.75 (s, 1H, O-H), 6.68–6.60 (m, 3H, Ar), 5.92 (s, 1H, =CH), 1.14 (s, 9H, *t*-Bu). <sup>13</sup>C NMR (CDCl<sub>3</sub>):  $\delta$  207.05, 161.94, 145.08, 139.59, 119.07, 107.32, 100.80, 92.22, 42.13, 25.75. Anal. Calcd for  $C_{14}H_{14}F_5NO$ : C, 54.73; H, 4.59; N, 4.56. Found: C, 54.79; H, 4.60; N, 4.51.

**2,3,4-F<sub>3</sub>PhN=C(CF<sub>3</sub>)CHC(*t*-Bu)OH (2k).** Compound **2k** was prepared via a procedure similar to that for **2b** as a light yellow oil in 78% yield. <sup>1</sup>H NMR (CDCl<sub>3</sub>):  $\delta$  11.38 (s, 1H, O-H), 7.07–6.91 (m, 2H, Ar), 6.01 (s, 1H, =CH) 1.22 (s, 9H, *t*-Bu). <sup>13</sup>C NMR

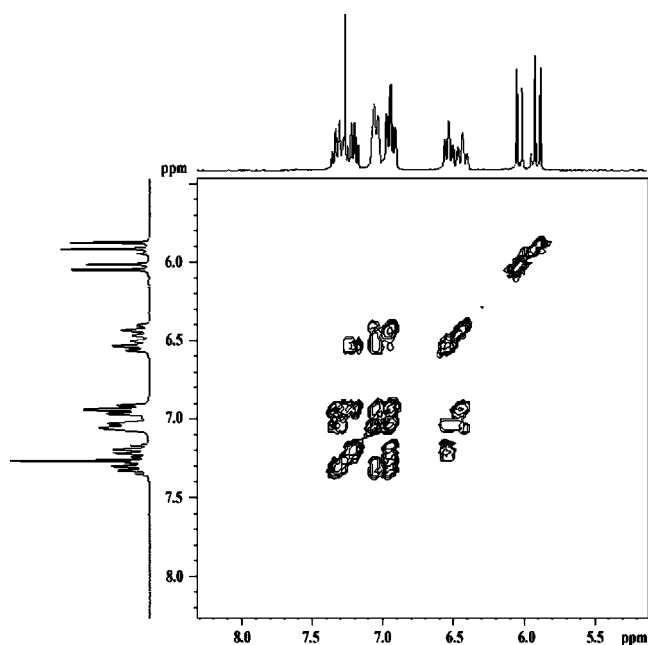


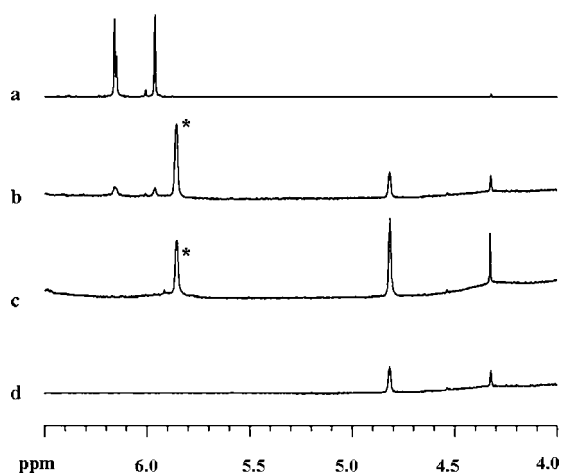
Figure 5. <sup>1</sup>H–<sup>1</sup>H COSY spectra of complex **4b**. The resonances at 5.8–6.2 ppm are for the methine protons of the ligands, and those at 6.4–7.4 ppm are for the aromatic protons.



Table 5. Polymerization of Ethylene by 4a–t/MMAO Systems<sup>a</sup>

entry	complex ( $\mu\text{mol}$ )	polymer (g)	activity <sup>b</sup>	$T_m^c$ ( $^\circ\text{C}$ )	$\bar{M}_n^d$ (kg/mol)	$\bar{M}_w/\bar{M}_n^d$
1	<b>4a</b> (1.0)	0.36	4.32	138.6	221	1.8
2	<b>4b</b> (1.0)	0.70	8.40	140.0	285	1.5
3	<b>4c</b> (1.0)	0.77	9.24	140.7	157	2.1
4	<b>4d</b> (1.0)	0.80	9.60	140.1	228	1.9
5	<b>4e</b> (1.0)	0.62	7.44	137.8	286	1.6
6	<b>4f</b> (1.0)	0.60	7.20	140.9	249	1.6
7	<b>4g</b> (1.0)	0.65	7.80	138.1	204	1.6
8	<b>4h</b> (1.0)	0.13	1.56	137.3	79.0	1.5
9	<b>4i</b> (1.0)	0.59	7.08	137.1	180	1.9
10	<b>4j</b> (1.0)	0.34	4.08	137.2	169	2.0
11	<b>4k</b> (1.0)	0.40	4.80	136.7	251	2.1
12	<b>4L</b> (1.0)	0.23	2.76	136.0	32.0	2.3
13	<b>4m</b> (10)	trace				
14	<b>4n</b> (1.0)	0.40	4.80	135.4	232	2.0
15	<b>4o</b> (1.0)	0.59	7.08	139.1	227	2.1
16	<b>4p</b> (1.0)	0.68	8.16	138.9	249	2.0
17	<b>4q</b> (1.0)	0.63	7.56	136.9	277	2.1
18	<b>4r</b> (1.0)	0.10	1.20	134.7		
19	<b>4s</b> (10)	0.03	0.036			
20	<b>4t</b> (10)	0.04	0.048			

<sup>a</sup> Reaction conditions: 1 atm of ethylene pressure, Al/Ti (mol ratio) = 2000, toluene 50 mL, polymerization for 5 min. <sup>b</sup> kg of PE/mmol<sub>Ti</sub>·h. <sup>c</sup> Melting temperature measured by DSC. <sup>d</sup> Number-average molecular weight and polydispersity index of the resultant polyethylene determined by GPC using polystyrene standard.



**Figure 6.** <sup>1</sup>H NMR spectra of **4b** (a); **4b**/dried-MMAO samples (b, c) [Al:Ti = 25 (b); Al:Ti = 50 (c)]; dried-MMAO (d) (room temperature, benzene-*d*<sub>6</sub>). Asterisks mark the methine proton (–CH=C–) signals of the alkyl complex generated. The resonances at 4.54, 4.82 ppm are for the protons of the dried MMAO, and those at 5.86–6.16 ppm are for the methane protons of the ligands.

(CDCl<sub>3</sub>):  $\delta$  208.43, 150.61, 148.08, 148.00, 140.45, 123.82, 123.46, 116.19, 111.45, 93.19, 43.43, 26.96. Anal. Calcd for C<sub>14</sub>H<sub>13</sub>F<sub>6</sub>NO: C, 51.70; H, 4.03; N, 4.31. Found: C, 51.79; H, 3.99; N, 4.35.

**3,4,5-F<sub>3</sub>PhN=C(CF<sub>3</sub>)CHC(*t*-Bu)OH (2l).** Compound **2l** was prepared via a procedure similar to that for **2b** as an off-white solid in 62% yield. <sup>1</sup>H NMR (CDCl<sub>3</sub>):  $\delta$  11.70 (s, 1H, O-H), 6.91–6.81 (m, 2H, Ar), 5.98 (s, 1H, =CH), 1.21 (s, 9H, *t*-Bu). <sup>13</sup>C NMR (CDCl<sub>3</sub>):  $\delta$  208.27, 150.88, 146.21, 138.69, 133.66, 119.98, 110.62, 92.93, 43.19, 26.84. Anal. Calcd for C<sub>14</sub>H<sub>13</sub>F<sub>6</sub>NO: C, 51.70; H, 4.03; N, 4.31. Found: C, 51.68; H, 3.97; N, 4.27.

***o*-CF<sub>3</sub>PhN=C(CF<sub>3</sub>)CHC(*t*-Bu)OH (2m).** Compound **2m** was prepared via a procedure similar to that for **2b** as a light yellow oil in 67% yield. <sup>1</sup>H NMR (CDCl<sub>3</sub>):  $\delta$  11.66 (s, 1H, O-H), 7.62–7.31 (m, 4H, Ar), 5.94 (s, 1H, =CH), 1.16 (s, 9H, *t*-Bu). <sup>13</sup>C NMR (CDCl<sub>3</sub>):  $\delta$  206.81, 146.05, 135.46, 131.37, 127.91, 125.94, 125.43, 125.15, 122.60, 119.05, 92.21, 42.06, 25.84. Anal. Calcd for C<sub>15</sub>H<sub>15</sub>F<sub>6</sub>NO: C, 53.10; H, 4.46; N, 4.13. Found: C, 53.28; H, 4.41; N, 4.08.

***m*-CF<sub>3</sub>PhN=C(CF<sub>3</sub>)CHC(*t*-Bu)OH (2n).** Compound **2n**

was prepared via a procedure similar to that for **2b** as a brown-yellow solid in 79% yield. <sup>1</sup>H NMR (CDCl<sub>3</sub>):  $\delta$  11.83 (s, 1H, O-H), 7.54–7.30 (m, 4H, Ar), 5.91 (s, 1H, =CH), 1.16 (s, 9H, *t*-Bu). <sup>13</sup>C NMR (CDCl<sub>3</sub>):  $\delta$  207.11, 145.89, 137.90, 130.74, 128.60, 127.81, 122.25, 121.57, 125.62, 115.49, 91.50, 42.14, 25.90. Anal. Calcd for C<sub>15</sub>H<sub>15</sub>F<sub>6</sub>NO: C, 53.10; H, 4.46; N, 4.13. Found: C, 53.24; H, 4.42; N, 4.09.

***p*-CF<sub>3</sub>PhN=C(CF<sub>3</sub>)CHC(*t*-Bu)OH (2o).** Compound **2o** was prepared via a procedure similar to that for **2b** as a deep yellow oil in 82% yield. <sup>1</sup>H NMR (CDCl<sub>3</sub>):  $\delta$  12.11 (s, 1H, O-H), 7.70–7.32 (dd, 4H, Ar), 6.02 (s, 1H, =CH), 1.24 (s, 9H, *t*-Bu). <sup>13</sup>C NMR (CDCl<sub>3</sub>):  $\delta$  207.16, 145.45, 140.66, 127.39, 125.27, 123.97, 123.04, 119.31, 92.09, 42.20, 25.87. Anal. Calcd for C<sub>15</sub>H<sub>15</sub>F<sub>6</sub>NO: C, 53.10; H, 4.46; N, 4.13. Found: C, 53.01; H, 4.49; N, 4.16.

***p*-ClPhN=C(CF<sub>3</sub>)CHC(*t*-Bu)OH (2p).** Compound **2p** was prepared via a procedure similar to that for **2b** as a light yellow oil in 86% yield. <sup>1</sup>H NMR (CDCl<sub>3</sub>):  $\delta$  11.72 (s, 1H, O-H), 7.25–7.04 (dd, 4H, Ar), 5.86 (s, 1H, =CH), 1.15 (s, 9H, *t*-Bu). <sup>13</sup>C NMR (CDCl<sub>3</sub>):  $\delta$  206.95, 146.34, 135.67, 131.56, 128.17, 126.20, 119.18, 90.66, 42.08, 26.11. Anal. Calcd for C<sub>14</sub>H<sub>15</sub>ClF<sub>3</sub>NO: C, 55.00; H, 4.95; N, 4.58. Found: C, 54.84; H, 4.90; N, 4.62.

***p*-IPhN=C(CF<sub>3</sub>)CHC(*t*-Bu)OH (2q).** Compound **2q** was prepared via a procedure similar to that for **2b** as a light yellow solid in 59% yield. <sup>1</sup>H NMR (CDCl<sub>3</sub>):  $\delta$  11.80 (s, 1H, O-H), 7.68–6.95 (dd, 4H, Ar), 5.93 (s, 1H, =CH), 1.21 (s, 9H, *t*-Bu). <sup>13</sup>C NMR (CDCl<sub>3</sub>):  $\delta$  207.86, 146.99, 138.11, 137.89, 127.48, 120.12, 91.82, 91.37, 43.04, 27.08. Anal. Calcd for C<sub>14</sub>H<sub>15</sub>F<sub>3</sub>INO: C, 42.34; H, 3.81; N, 3.53. Found: C, 42.51; H, 3.77; N, 3.58.

***p*-O<sub>2</sub>NPhN=C(CF<sub>3</sub>)CHC(*t*-Bu)OH (2r).** Compound **2r** was prepared via a procedure similar to that for **2b** as a brown oil in 57% yield. <sup>1</sup>H NMR (CDCl<sub>3</sub>):  $\delta$  11.95 (s, 1H, O-H), 8.13–7.20 (dd, 4H, Ar), 6.01 (s, 1H, =CH), 1.12 (s, 9H, *t*-Bu). <sup>13</sup>C NMR (CDCl<sub>3</sub>):  $\delta$  208.75, 145.56, 145.29, 144.74, 125.21, 123.93, 120.50, 95.46, 44.37, 27.14. Anal. Calcd for C<sub>14</sub>H<sub>15</sub>F<sub>3</sub>N<sub>2</sub>O<sub>3</sub>: C, 53.17; H, 4.78; N, 8.86. Found: C, 53.32; H, 4.73; N, 8.82.

**PhCH<sub>2</sub>N=C(CF<sub>3</sub>)CHC(*t*-Bu)OH (2s).** Compound **2s** was prepared via a procedure similar to that for **2b** as colorless oil in 46% yield. <sup>1</sup>H NMR (CDCl<sub>3</sub>):  $\delta$  10.38 (s, 1H, O-H), 7.34–7.17 (m, 5H, Ph), 5.68 (s, 1H, =CH), 4.42 (d, 2H, CH<sub>2</sub>), 1.08 (s, 9H, *t*-Bu). <sup>13</sup>C NMR (CDCl<sub>3</sub>):  $\delta$  207.09, 148.63, 137.19, 128.87, 127.88, 127.39, 120.38, 88.78, 48.14, 42.67, 27.19. Anal. Calcd for C<sub>15</sub>H<sub>18</sub>F<sub>3</sub>NO: C, 63.15; H, 6.36; N, 4.91. Found: C, 63.35; H, 6.41; N, 4.94.

Table 6. Polymerization of Ethylene by Some Selected Catalytic Systems<sup>a</sup>

entry	complex	complex dosage ( $\mu$ mol)	ethylene pressure (atm)	time (min)	yield (g)	activity <sup>b</sup>
1	4d	1.0	2	5	1.23	14.7
2	4d	1.0	4	5	1.60	19.2
3	4k	1.0	2	5	0.50	6.0
4	4k	1.0	4	5	0.70	8.4
5	4b	0.2	1	5	0.14	8.40
6	4b	0.5	1	5	0.40	9.60
7	4b	1.0	1	5	0.70	8.40
8	4k	0.5	1	5	0.082	1.97
9	4k	1.0	1	5	0.40	4.80
10	4k	2.0	1	5	0.50	3.0
11	4b	1.0	4	5	0.88	10.5
12	4c	1.0	4	5	1.13	13.6
13	4f	1.0	4	5	0.84	10.1
14	4j	1.0	4	5	0.60	7.2
15	4b	0.5	1	10	0.74	8.9
16	4b	0.5	1	15	0.92	7.4
17	4k	0.5	1	10	0.13	1.56
18	4k	0.5	1	15	0.15	1.20

<sup>a</sup> Reaction conditions: Al/Ti (mol ratio) = 2000, toluene 50 mL. <sup>b</sup> kg of PE/mmole $\cdot$ h.

**C<sub>6</sub>H<sub>11</sub>N=C(CF<sub>3</sub>)CHC(*t*-Bu)OH (2t).** According to the literature,<sup>27</sup> to a well-stirred solution of 1,1,1-trifluoro-5,5-dimethyl-2,4-hexanedione (4.9 g, 25 mmol) and cyclohexylamine (14.3 mL, 125 mmol) in dry toluene (100 mL) under N<sub>2</sub> was added dropwise TiCl<sub>4</sub> (2.0 mL, 18.75 mmol) in 30 mL of dry toluene over a period of 1 h. The dark brown reaction mixture was stirred for 1 h and then heated to 130 °C overnight. After being cooled to room temperature, the reaction mixture was diluted with ether (200 mL) and was stirred until the color of the precipitate totally changed to light yellow. The mixture was filtered through Celite, and the collected precipitate was washed with ether. Concentration of the combined filtrate and washes gave the crude product, which was fractionated, giving a 35% yield of the ligand as a light yellow oil, boiling at 98 °C at 4 mmHg. <sup>1</sup>H NMR (CDCl<sub>3</sub>):  $\delta$  10.46 (s, 1H, O-H), 5.62 (s, 1H, =CH), 3.44 (s, 1H, CH), 1.95–1.30 (m, 10H, CH<sub>2</sub>), 1.16 (s, 9H, *t*-Bu). <sup>13</sup>C NMR (CDCl<sub>3</sub>):  $\delta$  205.56, 147.25, 119.22, 86.18, 52.31, 41.32, 33.49, 26.14, 24.09, 23.41. Anal. Calcd for C<sub>14</sub>H<sub>22</sub>F<sub>3</sub>N<sub>2</sub>O: C, 60.63; H, 8.00; N, 5.05. Found: C, 60.47; H, 7.94; N, 5.01.

**Synthesis of Titanium Complexes 4b–t.** [*o*-FPhN=C(CF<sub>3</sub>)CHC(*t*-Bu)O]<sub>2</sub>TiCl<sub>2</sub> (**4b**). To a stirred solution of compound *o*-FPhN=C(CF<sub>3</sub>)C(H)C(*t*-Bu)OH (**2b**, 1.16 g, 4 mmol) in dried diethyl ether (20 mL) at –78 °C was added dropwise a 1.6 M *n*-butyllithium hexane solution (2.5 mL, 4 mmol) over 5 min. The mixture was allowed to warm to room temperature and stirred for 2.5 h. Then the mixture was added dropwise to TiCl<sub>4</sub> (2 mmol) in dried diethyl ether (30 mL) at –78 °C with stirring over 30 min. The mixture was allowed to warm to room temperature and stirred overnight. The evaporation of the solvent under vacuum yielded a crude product. To the crude product was added 30 mL of dried hexane, and the mixture was stirred for 10 min at 60 °C and then filtered. The deep red solution was cooled to –35 °C slowly to give red crystals (0.89 g) in 67% yield as the product. <sup>1</sup>H NMR (CDCl<sub>3</sub>):  $\delta$  7.30–6.92 (m, 8H, Ar), 6.00–5.79 (q, 2H, =CH), 0.95 (q, 18H, *t*-Bu). <sup>13</sup>C NMR (CDCl<sub>3</sub>): 195.13, 160.24, 155.34, 136.78, 129.79, 128.70, 125.55, 123.74, 116.77, 98.91, 40.89, 28.11. <sup>19</sup>F NMR (CDCl<sub>3</sub>):  $\delta$  –63.5, –63.2, –63.1, –115.5, –117.9, –118.4, –121.1. Anal. Calcd for C<sub>28</sub>H<sub>28</sub>Cl<sub>2</sub>F<sub>8</sub>N<sub>2</sub>O<sub>2</sub>Ti: C, 48.37; H, 4.06; N, 4.03. Found: C, 48.48; H, 4.01; N, 4.08.

[*m*-FPhN=C(CF<sub>3</sub>)CHC(*t*-Bu)O]<sub>2</sub>TiCl<sub>2</sub> (**4c**). Complex **4c** was prepared via a procedure similar to that for **4b** as red crystals in 78% yield. <sup>1</sup>H NMR (CDCl<sub>3</sub>):  $\delta$  7.33–6.42 (m, 8H, Ar), 6.05–5.88 (q, 2H, =CH), 1.02 (q, 18H, *t*-Bu). <sup>13</sup>C NMR (CDCl<sub>3</sub>): 194.29, 163.64, 158.12, 148.73, 129.63, 122.54, 119.67, 114.76, 110.12,

98.31, 40.47, 27.67. <sup>19</sup>F NMR (300 MHz, CDCl<sub>3</sub>):  $\delta$  –60.7, –60.6, –112.9, –111.5, –111.3, –111.2. Anal. Calcd for C<sub>28</sub>H<sub>28</sub>Cl<sub>2</sub>F<sub>8</sub>N<sub>2</sub>O<sub>2</sub>Ti: C, 48.37; H, 4.06; N, 4.03. Found: C, 48.51; H, 4.03; N, 3.98.

[*p*-FPhN=C(CF<sub>3</sub>)CHC(*t*-Bu)O]<sub>2</sub>TiCl<sub>2</sub> (**4d**). Complex **4d** was prepared via a procedure similar to that for **4b** as red crystals in 76% yield. <sup>1</sup>H NMR (CDCl<sub>3</sub>): 7.18–6.50 (m, 8H, Ar), 5.88 (s, 1H, =CH), 0.95 (s, 18H, *t*-Bu). <sup>13</sup>C NMR (CDCl<sub>3</sub>): 194.13, 161.01, 158.26, 143.29, 128.36, 123.45, 120.05, 115.60, 114.92, 98.28, 40.31, 27.65. <sup>19</sup>F NMR (CDCl<sub>3</sub>):  $\delta$  –52.1, –109.9. Anal. Calcd for C<sub>28</sub>H<sub>28</sub>Cl<sub>2</sub>F<sub>8</sub>N<sub>2</sub>O<sub>2</sub>Ti: C, 48.37; H, 4.06; N, 4.03. Found: C, 48.19; H, 4.01; N, 3.99.

[2,3-F<sub>2</sub>PhN=C(CF<sub>3</sub>)CHC(*t*-Bu)O]<sub>2</sub>TiCl<sub>2</sub> (**4e**). Complex **4e** was prepared via a procedure similar to that for **4b** as red crystals in 73% yield. <sup>1</sup>H NMR (CDCl<sub>3</sub>):  $\delta$  7.15–6.80 (t, 1H, Ar), 6.20–5.83 (q, 2H, =CH), 1.02 (q, 18H, *t*-Bu). <sup>13</sup>C NMR (CDCl<sub>3</sub>): 195.88, 159.74, 152.36, 143.73, 137.41, 136.56, 124.35, 122.89, 120.67, 98.64, 40.77, 27.62. <sup>19</sup>F NMR (CDCl<sub>3</sub>):  $\delta$  –63.0, –63.4, –136.1, –137.4, –138.6, –145.5. Anal. Calcd for C<sub>28</sub>H<sub>26</sub>Cl<sub>2</sub>F<sub>10</sub>N<sub>2</sub>O<sub>2</sub>Ti: C, 45.99; H, 3.58; N, 3.83. Found: C, 45.83; H, 3.59; N, 3.78.

[2,4-F<sub>2</sub>PhN=C(CF<sub>3</sub>)CHC(*t*-Bu)O]<sub>2</sub>TiCl<sub>2</sub> (**4f**). Complex **4f** was prepared via a procedure similar to that for **4b** as red crystals in 84% yield. <sup>1</sup>H NMR (CDCl<sub>3</sub>):  $\delta$  7.28–6.66 (m, 6H, Ar), 6.04–5.84 (q, 1H, =CH), 0.98 (q, 18H, *t*-Bu). <sup>13</sup>C NMR (CDCl<sub>3</sub>): 195.37, 162.96, 160.27, 155.38, 130.11, 125.68, 120.65, 110.34, 104.97, 98.17, 40.65, 27.69. <sup>19</sup>F NMR (CDCl<sub>3</sub>):  $\delta$  –63.1, –63.5, –110.4, –10.9, –111.1, –112.8. Anal. Calcd for C<sub>28</sub>H<sub>26</sub>Cl<sub>2</sub>F<sub>10</sub>N<sub>2</sub>O<sub>2</sub>Ti: C, 45.99; H, 3.58; N, 3.83. Found: C, 45.92; H, 3.56; N, 3.79.

[2,5-F<sub>2</sub>PhN=C(CF<sub>3</sub>)CHC(*t*-Bu)O]<sub>2</sub>TiCl<sub>2</sub> (**4g**). Complex **4g** was prepared via a procedure similar to that for **4b** as red crystals in 65% yield. <sup>1</sup>H NMR (CDCl<sub>3</sub>):  $\delta$  7.15–6.72 (m, 6H, Ar), 6.05, 6.02 (d, 2H, =CH), 1.06 (q, 18H, *t*-Bu). <sup>13</sup>C NMR (CDCl<sub>3</sub>): 195.89, 160.06, 156.14, 149.84, 137.05, 120.16, 116.84, 115.83, 114.40, 98.37, 40.83, 27.71. <sup>19</sup>F NMR (CDCl<sub>3</sub>):  $\delta$  –63.3, –63.6, –117.2, –118.4, –121.8, –124.6. Anal. Calcd for C<sub>28</sub>H<sub>26</sub>Cl<sub>2</sub>F<sub>10</sub>N<sub>2</sub>O<sub>2</sub>Ti: C, 45.99; H, 3.58; N, 3.83. Found: C, 46.12; H, 3.54; N, 3.78.

[2,6-F<sub>2</sub>PhN=C(CF<sub>3</sub>)CHC(*t*-Bu)O]<sub>2</sub>TiCl<sub>2</sub> (**4h**). Complex **4h** was prepared via a procedure similar to that for **4b** as a red solid in 80% yield. <sup>1</sup>H NMR (CDCl<sub>3</sub>):  $\delta$  7.13–6.76 (m, 6H, Ar), 5.98 (s, 1H, =CH), 0.98 (s, 18H, *t*-Bu). <sup>13</sup>C NMR (CDCl<sub>3</sub>): 194.78, 160.05, 155.22, 126.95, 125.78, 117.59, 110.98, 110.70, 110.72, 97.51, 39.70, 26.61. <sup>19</sup>F NMR (CDCl<sub>3</sub>):  $\delta$  –65.9, –112.4, –113.8. Anal. Calcd for C<sub>28</sub>H<sub>26</sub>Cl<sub>2</sub>F<sub>10</sub>N<sub>2</sub>O<sub>2</sub>Ti: C, 45.99; H, 3.58; N, 3.83. Found: C, 45.74; H, 3.54; N, 3.87.

[3,4-F<sub>2</sub>PhN=C(CF<sub>3</sub>)CHC(*t*-Bu)O]<sub>2</sub>TiCl<sub>2</sub> (**4i**). Complex **4i** was prepared via a procedure similar to that for **4b** as red crystals in 67% yield. <sup>1</sup>H NMR (CDCl<sub>3</sub>):  $\delta$  7.20–6.41 (m, 6H, Ar), 6.08–5.92

(27) Siemens. ASTRO, SAINT, and SADABS. Data Collection and Processing Software for the SMART System; Siemens Analytical X-ray Instruments Inc.: Madison, WI, 1996.

(q, 2H, =CH), 1.06 (q, 18H, *t*-Bu).  $^{13}\text{C}$  NMR ( $\text{CDCl}_3$ ): 195.26, 159.95, 152.23, 147.26, 143.72, 123.24, 121.24, 118.51, 116.80, 112.29, 40.91, 27.92.  $^{19}\text{F}$  NMR ( $\text{CDCl}_3$ ):  $\delta$  -60.4, -134.6, -136.3, -138.9. Anal. Calcd for  $\text{C}_{28}\text{H}_{26}\text{Cl}_2\text{F}_{10}\text{N}_2\text{O}_2\text{Ti}$ : C, 45.99; H, 3.58; N, 3.83. Found: C, 45.81; H, 3.53; N, 3.86.

**[3,5-F<sub>2</sub>PhN=C(CF<sub>3</sub>)CHC(*t*-Bu)O]<sub>2</sub>TiCl<sub>2</sub> (4j).** Complex **4j** was prepared via a procedure similar to that for **4b** as red crystals in 65% yield.  $^1\text{H}$  NMR ( $\text{CDCl}_3$ ):  $\delta$  6.77 (d, 2H, Ar), 6.63 (t, 2H, Ar), 6.12 (d, 2H, Ar), 5.94 (s, 2H, =CH), 1.00 (q, 18H, *t*-Bu).  $^{13}\text{C}$  NMR ( $\text{CDCl}_3$ ): 195.10, 163.85, 160.54, 158.52, 149.27, 120.87, 110.90, 106.36, 102.44, 98.29, 40.58, 27.63.  $^{19}\text{F}$  NMR ( $\text{CDCl}_3$ ):  $\delta$  -60.7, -107.9, -109.9. Anal. Calcd for  $\text{C}_{28}\text{H}_{26}\text{Cl}_2\text{F}_{10}\text{N}_2\text{O}_2\text{Ti}$ : C, 45.99; H, 3.58; N, 3.83. Found: C, 45.78; H, 3.55; N, 3.79.

**[2,3,4-F<sub>3</sub>PhN=C(CF<sub>3</sub>)CHC(*t*-Bu)O]<sub>2</sub>TiCl<sub>2</sub> (4k).** Complex **4k** was prepared via a procedure similar to that for **4b** as red crystals in **4k** in 67% yield.  $^1\text{H}$  NMR ( $\text{CDCl}_3$ ):  $\delta$  7.08–6.86 (m, 4H, Ar), 6.23–5.88 (q, 2H, =CH), 1.11 (q, 18H, *t*-Bu).  $^{13}\text{C}$  NMR ( $\text{CDCl}_3$ ): 196.85, 160.63, 151.93, 148.56, 133.25, 123.20, 120.97, 117.17, 111.26, 98.72, 41.27, 27.98.  $^{19}\text{F}$  NMR ( $\text{CDCl}_3$ ):  $\delta$  -62.9, -63.1, -63.5, -133.0, -134.6, -139.3, -157.0, -159.3. Anal. Calcd for  $\text{C}_{28}\text{H}_{24}\text{Cl}_2\text{F}_{12}\text{N}_2\text{O}_2\text{Ti}$ : C, 43.83; H, 3.15; N, 3.65. Found: C, 43.71; H, 3.09; N, 3.68.

**[3,4,5-F<sub>3</sub>PhN=C(CF<sub>3</sub>)CHC(*t*-Bu)O]<sub>2</sub>TiCl<sub>2</sub> (4l).** Complex **4l** was prepared via a procedure similar to that for **4b** as red crystals in 70% yield.  $^1\text{H}$  NMR ( $\text{CDCl}_3$ ):  $\delta$  6.97 (m, 2H, Ar), 6.24 (m, 2H, Ar), 6.05 (s, 2H, =CH), 1.10 (s, 18H, *t*-Bu).  $^{13}\text{C}$  NMR ( $\text{CDCl}_3$ ): 196.05, 159.38, 152.66, 149.23, 142.66, 138.99, 114.85, 112.40, 107.72, 98.57, 40.99, 27.90.  $^{19}\text{F}$  NMR ( $\text{CDCl}_3$ ):  $\delta$  -60.5, -131.7, -132.6, -133.6, -161.1. Anal. Calcd for  $\text{C}_{28}\text{H}_{24}\text{Cl}_2\text{F}_{12}\text{N}_2\text{O}_2\text{Ti}$ : C, 43.83; H, 3.15; N, 3.65. Found: C, 43.67; H, 3.10; N, 3.61.

**[o-CF<sub>3</sub>PhN=C(CF<sub>3</sub>)CHC(*t*-Bu)O]<sub>2</sub>TiCl<sub>2</sub> (4m).** Complex **4m** was prepared via a procedure similar to that for **4b** as red crystals in 76% yield.  $^1\text{H}$  NMR ( $\text{CDCl}_3$ ):  $\delta$  7.69–7.33 (m, 8H, Ar), 6.01 (s, 2H, =CH), 0.89 (s, 18H, *t*-Bu).  $^{13}\text{C}$  NMR ( $\text{CDCl}_3$ ): 195.34, 157.68, 145.18, 136.43, 132.43, 131.17, 129.51, 128.23, 125.39, 119.38, 98.86, 41.02, 27.66.  $^{19}\text{F}$  NMR ( $\text{CDCl}_3$ ):  $\delta$  -61.0, -62.5. Anal. Calcd for  $\text{C}_{30}\text{H}_{28}\text{Cl}_2\text{F}_{12}\text{N}_2\text{O}_2\text{Ti}$ : C, 45.31; H, 3.55; N, 3.52. Found: C, 45.21; H, 3.51; N, 3.47.

**[*m*-CF<sub>3</sub>PhN=C(CF<sub>3</sub>)CHC(*t*-Bu)O]<sub>2</sub>TiCl<sub>2</sub> (4n).** Complex **4n** was prepared via a procedure similar to that for **4b** as red crystals in 82% yield.  $^1\text{H}$  NMR ( $\text{CDCl}_3$ ):  $\delta$  7.61–6.92 (m, 8H, Ar), 5.98 (q, 2H, =CH), 0.95 (q, 18H, *t*-Bu).  $^{13}\text{C}$  NMR ( $\text{CDCl}_3$ ): 194.50, 158.69, 147.83, 131.05, 130.62, 129.65, 125.29, 123.57, 120.69, 118.02, 98.12, 40.44, 27.40. Anal. Calcd for  $\text{C}_{30}\text{H}_{28}\text{Cl}_2\text{F}_{12}\text{N}_2\text{O}_2\text{Ti}$ : C, 45.31; H, 3.55; N, 3.52. Found: C, 45.18; H, 3.52; N, 3.48.

**[*p*-CF<sub>3</sub>PhN=C(CF<sub>3</sub>)CHC(*t*-Bu)O]<sub>2</sub>TiCl<sub>2</sub> (4o).** Complex **4o** was prepared via a procedure similar to that for **4b** as red crystals in 86% yield.  $^1\text{H}$  NMR ( $\text{CDCl}_3$ ):  $\delta$  7.55 (d, 2H, Ar), 7.50 (d, 2H, Ar), 7.32 (d, 2H, Ar), 6.77 (d, 2H, Ar), 5.88 (s, 2H, =CH), 0.90 (s, 18H, *t*-Bu).  $^{13}\text{C}$  NMR ( $\text{CDCl}_3$ ): 194.84, 158.20, 150.40, 129.20, 127.28, 125.76, 125.53, 125.24, 122.43, 118.29, 98.27, 40.41, 27.48.  $^{19}\text{F}$  NMR ( $\text{CDCl}_3$ ):  $\delta$  -60.3, -62.0. Anal. Calcd for  $\text{C}_{30}\text{H}_{28}\text{Cl}_2\text{F}_{12}\text{N}_2\text{O}_2\text{Ti}$ : C, 45.31; H, 3.55; N, 3.52. Found: C, 45.19; H, 3.52; N, 3.47.

**[*p*-CIPhN=C(CF<sub>3</sub>)CHC(*t*-Bu)O]<sub>2</sub>TiCl<sub>2</sub> (4p).** Complex **4p** was prepared via a procedure similar to that for **4b** as red crystals in 71% yield.  $^1\text{H}$  NMR ( $\text{CDCl}_3$ ):  $\delta$  7.24 (d, 2H, Ar), 7.22 (m, 4H, Ar), 6.55 (d, 2H, Ar), 5.88 (s, 1H, =CH), 0.95 (s, 18H, *t*-Bu).  $^{13}\text{C}$  NMR ( $\text{CDCl}_3$ ): 194.79, 158.55, 146.21, 132.88, 129.05, 128.43, 123.61, 119.25, 98.74, 40.72, 27.99.  $^{19}\text{F}$  NMR ( $\text{CDCl}_3$ ):  $\delta$  -60.3. Anal. Calcd for  $\text{C}_{28}\text{H}_{28}\text{Cl}_2\text{F}_6\text{N}_2\text{O}_2\text{Ti}$ : C, 46.18; H, 3.88; N, 3.85. Found: C, 46.02; H, 3.83; N, 3.88.

**[*p*-IPhN=C(CF<sub>3</sub>)CHC(*t*-Bu)O]<sub>2</sub>TiCl<sub>2</sub> (4q).** Complex **4q** was prepared via a procedure similar to that for **4b** as red crystals in 76% yield.  $^1\text{H}$  NMR ( $\text{CDCl}_3$ ):  $\delta$  7.67 (d, 2H, Ar), 7.02 (m, 4H, Ar), 6.45 (d, 2H, Ar), 5.93 (s, 1H, =CH), 1.04 (s, 18H, *t*-Bu).  $^{13}\text{C}$  NMR ( $\text{CDCl}_3$ ): 194.85, 158.36, 147.48, 137.93, 137.32, 129.11, 124.28,

119.35, 98.75, 92.02, 40.77, 28.05.  $^{19}\text{F}$  NMR ( $\text{CDCl}_3$ ):  $\delta$  -60.3. Anal. Calcd for  $\text{C}_{28}\text{H}_{28}\text{Cl}_2\text{F}_6\text{N}_2\text{O}_2\text{Ti}$ : C, 36.91; H, 3.10; N, 3.07. Found: C, 36.78; H, 3.04; N, 3.03.

**[*p*-O<sub>2</sub>NPhN=C(CF<sub>3</sub>)CHC(*t*-Bu)O]<sub>2</sub>TiCl<sub>2</sub> (4r).** Complex **4r** was prepared via a procedure similar to that for **4b** as red crystals in 66% yield.  $^1\text{H}$  NMR ( $\text{CDCl}_3$ ):  $\delta$  6.77 (d, 2H, Ar), 6.63 (t, 2H, Ar), 6.12 (d, 2H, Ar), 5.94 (s, 1H, =CH), 1.00 (s, 18H, *t*-Bu).  $^{19}\text{F}$  NMR ( $\text{CDCl}_3$ ):  $\delta$  -60.3. Anal. Calcd for  $\text{C}_{28}\text{H}_{28}\text{Cl}_2\text{F}_6\text{N}_4\text{O}_6\text{Ti}$ : C, 44.88; H, 3.77; N, 7.48. Found: C, 44.62; H, 3.73; N, 7.53.

**[PhCH<sub>2</sub>N=C(CF<sub>3</sub>)CHC(*t*-Bu)O]<sub>2</sub>TiCl<sub>2</sub> (4s).** Complex **4s** was prepared via a procedure similar to that for **4b** as a black solid in 73% yield.  $^1\text{H}$  NMR ( $\text{CDCl}_3$ ):  $\delta$  7.39–7.07 (m, 10H, Ar), 6.11 (s, 2H, =CH), 4.87 (d, 2H, CH<sub>2</sub>), 4.65 (d, 2H, CH<sub>2</sub>), 5.94 (s, 1H, =CH), 1.04 (q, 18H, *t*-Bu).  $^{13}\text{C}$  NMR ( $\text{CDCl}_3$ ): 194.01, 160.27, 138.13, 128.55, 127.23, 126.56, 121.27, 99.34, 58.26, 40.56, 27.86.  $^{19}\text{F}$  NMR ( $\text{CDCl}_3$ ):  $\delta$  -62.6. Anal. Calcd for  $\text{C}_{30}\text{H}_{34}\text{Cl}_2\text{F}_6\text{N}_2\text{O}_2\text{Ti}$ : C, 52.42; H, 4.99; N, 4.08. Found: C, 52.29; H, 4.95; N, 4.03.

**[C<sub>6</sub>H<sub>11</sub>N=C(CF<sub>3</sub>)CHC(*t*-Bu)O]<sub>2</sub>TiCl<sub>2</sub> (4t).** Complex **4t** was prepared via a procedure similar to that for **4b** as red crystals in 61%.  $^1\text{H}$  NMR ( $\text{CDCl}_3$ ):  $\delta$  6.29 (s, 2H, =CH), 3.85 (s, 2H, CH), 2.05–1.35 (m, 20H, CH<sub>2</sub>), 1.05 (s, 18H, *t*-Bu).  $^{19}\text{F}$  NMR ( $\text{CDCl}_3$ ):  $\delta$  -61.1. Anal. Calcd for  $\text{C}_{28}\text{H}_{42}\text{Cl}_2\text{F}_6\text{N}_2\text{O}_2\text{Ti}$ : C, 50.09; H, 6.31; N, 4.17. Found: C, 49.86; H, 6.25; N, 4.24.

**X-ray Crystallography.** Single crystals of complexes **4a–d**, **4j**, and **4m** suitable for X-ray structure determination were grown from a hexane solution at -20 °C in a glovebox, thus maintaining a dry, O<sub>2</sub>-free environment. X-ray intensities of complexes **4a–d**, **4j**, and **4m** were collected on a Bruker Smart CCD diffractometer equipped with graphite-monochromated Mo K $\alpha$  radiation ( $\lambda$  = 0.71073 Å) at 187 K. Empirical absorption corrections were applied to the data using the SADABS program.<sup>28</sup> The structures were solved by the direct method and refined by full-matrix least-squares on  $F^2$  using the SHELXTL-97 program.<sup>29</sup> All of the non-hydrogen atoms were refined anisotropically. Crystallographic data and other pertinent information for **4a–d**, **4j**, and **4m** are summarized in Table 2. Selected bond lengths and angles are listed in Table 3.

**Computational Details.** Initial conformations of **4a–d**, **4j**, and **4m** were obtained from their crystal data collected on an X-ray diffractometer and taken as input structures for geometry optimization in the Amsterdam Density Functional program package (ADF 2006.1b).<sup>30</sup> The thus located low-energy conformers were modified to build the initial structures of isomers and other catalysts, which are optimized in ADF again. The calculations were carried out at the level of gradient-corrected density functional theory using the Becke–Perdew exchange–correlation functional.<sup>31</sup> A standard double STO basis set with polarization function (DZP) was employed for all atoms except Ti, which was described by a triple- $\xi$  plus polarization STO basis (TZP). The frozen core approximation was employed for the 1s electrons of the C, O, and F atoms, up to and including the 2p of the Cl atoms and the 3p electrons of Ti. All stationary points were optimized without any symmetry and geometry constraints. Numerical integrations were performed with the integration precision of 4.0, and the default ADF values were chosen for the self-consistent-field (SCF) and geometry optimization convergence criteria.

(28) Sheldrick, G. M. *SHELXL-97, A Program for Crystal Structure Refinement*; University of Göttingen: Göttingen, Germany, 1997.

(29) (a) Denmark, S. E.; Rivera, I. *J. Org. Chem.* **1994**, *59*, 6887–6889. (b) Dai, W.; Srinivasan, R.; Katzenellenbogen, J. A. *J. Org. Chem.* **1989**, *54*, 2204–2208.

(30) (a) *ADF2006.01*; SCM, Theoretical Chemistry, Vrije Universiteit: Amsterdam, The Netherlands. (b) te Velde, G.; Bickelhaupt, F. M.; van Gisbergen, S. J. A.; Fonseca Guerra, C.; Baerends, E. J.; Snijders, J. G.; Ziegler, T. *J. Comput. Chem.* **2001**, *22*, 931. (c) Fonseca Guerra, C.; Snijders, J. G.; te Velde, G.; Baerends, E. J. *Theor. Chem. Acc.* **1998**, *99*, 391.

(31) (a) Becke, A. *Phys. Rev. A* **1988**, *38*, 3098. (b) Perdew, J. P. *Phys. Rev. B* **1986**, *34*, 7406–7406. (c) Perdew, J. P. *Phys. Rev. B* **1986**, *33*, 8822.

**Ethylene Polymerization.** Polymerization was carried out under atmospheric pressure in toluene in a 150 mL glass reactor equipped with a mechanical stirrer. Toluene (50 mL) was introduced into the argon-purged reactor and stirred vigorously (600 rpm). The toluene was kept at a prescribed polymerization temperature, and then the ethylene gas feed was started. After 15 min, the polymerization was initiated by the addition of a heptane solution of MMAO and a toluene solution of one of the titanium complexes into the reactor with vigorous stirring (600 rpm). After a prescribed time, isobutyl alcohol (10 mL) was added to terminate the polymerization reaction, and the ethylene gas feed was stopped. The resulting mixture was added to the acidic methanol. The solid polyethylene was isolated by filtration, washed with methanol, and dried at 60 °C for 24 h in a vacuum oven.

**Study of the Active Intermediates by  $^1\text{H}$  NMR.** A solution of **4b** (3.5 mg, 5  $\mu\text{mol}$ ) in benzene- $d_6$  was added dropwise to a solution of dried MMAO (7.3 mg, 125  $\mu\text{mol}$  or 14.6 mg, 250  $\mu\text{mol}$ ) in benzene- $d_6$ . The resulting mixture was shaken and was then

transferred into a Young's Teflon NMR tube to measure the  $^1\text{H}$  NMR spectroscopic data at room temperature (25 °C).

**Acknowledgment.** The authors are grateful for a subsidy provided by the National Natural Science Foundation of China (Nos. 20734002 and 50525312) and by the Special Funds for Major State Basis Research Projects (No. 2005CB623800) from the Ministry of Science and Technology of China.

**Supporting Information Available:** CIF files giving complete X-ray experimental details and tables of bond lengths, angles, and positional parameters for complexes **4a–d**, **4j**, and **4m**. The molecular structures of **4c**, **4d**, and **4j** are shown in Figures S1–S3, respectively. These materials are available free of charge via the Internet at <http://pubs.acs.org>.

OM700803U